Nucleosynthesis in classical novae

Margarita Hernanz

Institut d'Estudis Espacials de Catalunya, IEEC-CSIC

Barcelona (Spain)

OUTLINE

- Scenario of nova explosions: thermonuclear runaway – Mixing between core and envelope material
- Properties of the underlying white dwarf: CO and ONe
- Theoretical models: general predictions as compared with observations
- Relevance of nucleosynthesis in classical novae:
  - chemical evolution of the Galaxy
  - presolar meteoritic grains
  - gamma-ray emission

Scenario

Mass transfer from the companion star onto the white dwarf (cataclysmic variable)

↓

Hydrogen burning in degenerate conditions on top of the white dwarf

↓

Thermonuclear runaway

↓

Explosive H-burning ↗

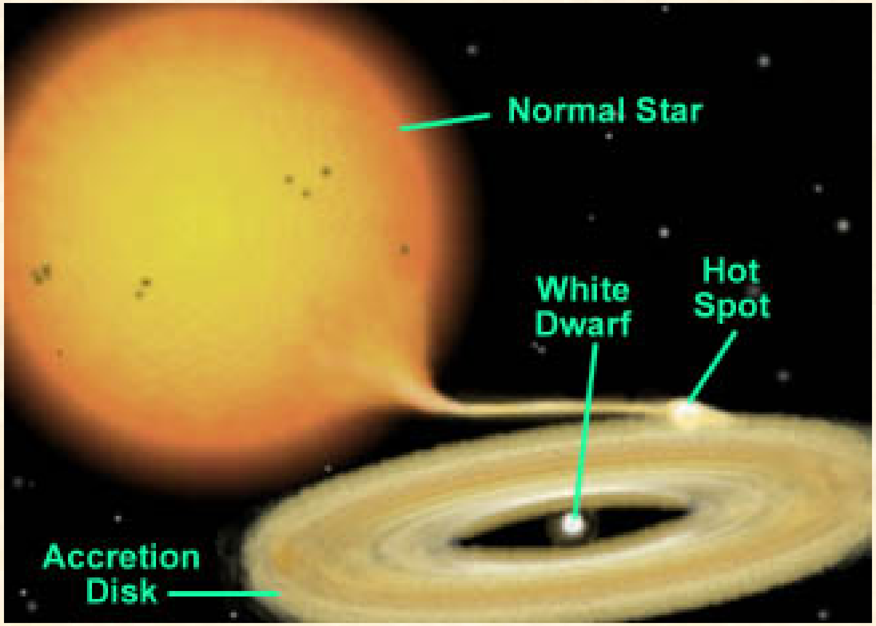

Decay of short-lived radioactive nuclei in the outer envelope (transported by convection)

↓

Envelope expansion, L increase and mass ejection

Nova Models: Thermonuclear Burning of Hydrogen. CNO cycle

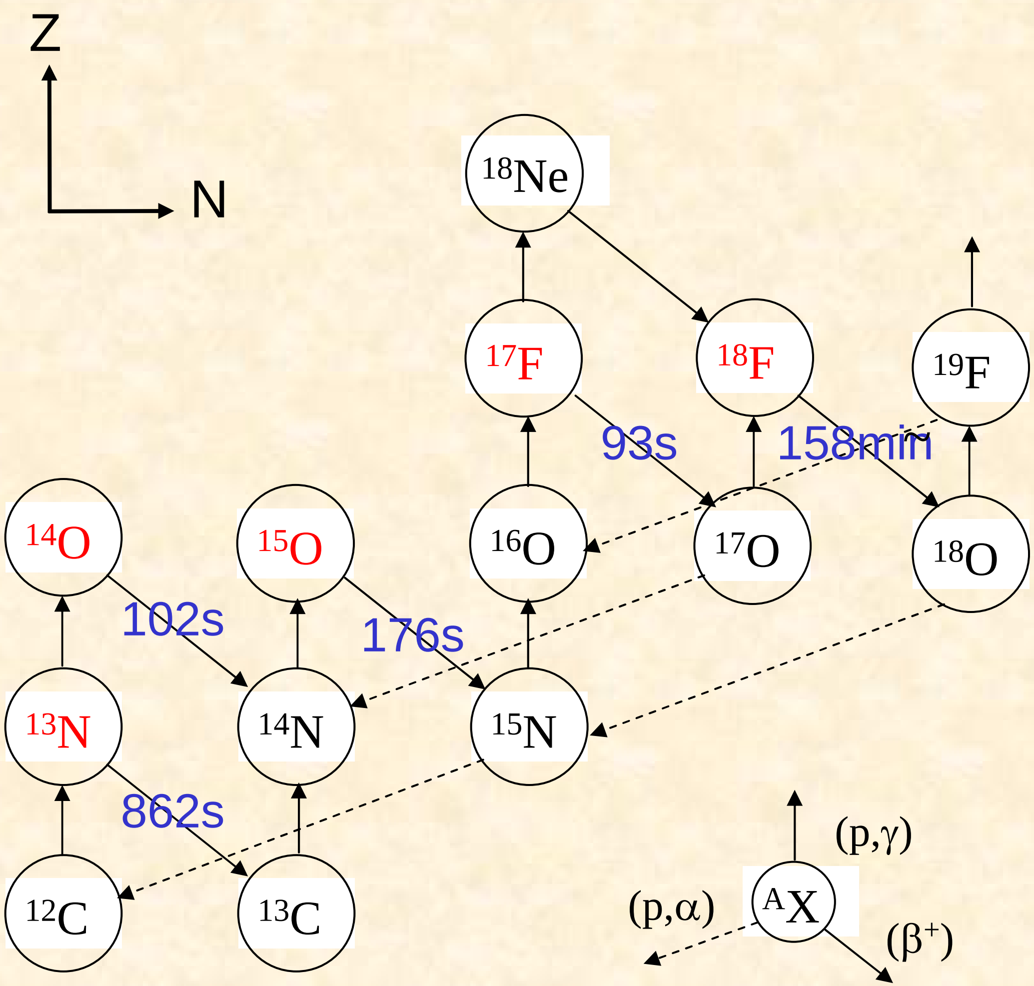

- Start: $\tau_{\beta+} < \tau(p,\gamma)$

  ↓

  CNO cycle operates in equ.
- T ~10^8 K: $\tau_{\beta+} > \tau(p,\gamma)$

  ↓

  CNO cycle β^+-limited (bottle neck)
- Convection:
  - fresh fuel brought to the burning shell
  - $\tau_{conv} < \tau_{\beta+}$: β^+-unstable nuclei to external cooler regions where they are preserved from destruction

Later decay on the surface leads to expansion and luminosity increase

Novae observations: spectra - abundances determinations

Expansion velocities ~ 10^2-10^3 km/s

Ejecta often enhanced in C, N, O, Ne

Metallicities >> Solar

Nova Abundances—Observations (Livio & Truran 1994)

Nova	Year	X	Y	Z	CNO/Z	C/N	O/N	O/(C + N)
T Aur	1891	0.47	0.40	0.13	1.00	...	0.65	0.65
RR Pic...........	1925	0.53	0.43	0.043	0.74	0.18	0.26	0.22
DQ Her	1934	0.27	0.16	0.57	1.00	0.20	0.76	0.63
		0.34	0.09	0.57	1.00	0.20	1.26	1.05
HR Del	1967	0.45	0.48	0.077	0.96	...	1.74[a]	1.74
V1500 Cyg	1975	0.49	0.21	0.30	0.92	0.93	1.73	0.90
		0.57	0.27	0.16	0.93	1.41[b]	1.22	0.51
V1688 Cyg	1978	0.45	0.22	0.33	1.00	0.50	0.86	0.57
		0.45	0.23	0.32	0.98	0.34	0.93	0.70
V693 CrA	1981	0.29	0.32	0.39	0.52[c]	0.06	1.50	1.42
V1370 Aql.......	1982	0.04	0.10	0.86	0.32[c]	0.06	0.19	0.15
GQ Mus	1983	0.27	0.32	0.41	0.97	0.08	1.00	0.93
PW Vul	1984	0.47	0.23	0.30	0.99	0.52	0.59	0.39
		0.54	0.28	0.18	1.00	0.29	0.35	0.27
		0.69	0.25	0.067	0.99	0.67	0.29	0.27
QU Vul	1984	0.33	0.26	0.40	0.63[c]	0.13	2.30	2.04
V842 Cen........	1986	0.41	0.23	0.36	0.99	0.57	0.14	0.09
V827 Her	1987	0.36	0.29	0.35	0.98	0.36	0.07	0.05
QV Vul	1987	0.68	0.27	0.053	0.96	...	4.10[a]	4.10
V2214 Oph......	1988	0.34	0.26	0.40	0.93	...	0.19	0.19
V977 Sco	1989	0.51	0.39	0.10	0.72	...	0.71	0.71
V443 Sct.........	1989	0.49	0.45	0.062	0.97	...	0.13	0.13
LMC.............	1990A	0.37	0.59	0.039	0.35[c]	0.08	0.82	0.76
					0.73	*3.1*	*9.7*	*2.4*	***SOLAR***

[a] Exceptionally high O/N and C/N ~ 0.
[b] Exception to C/N < 1.
[c] Novae with low CNO/Z ratios—probably ONeMg progenitors.

C/N<1

TABLE 2

Heavy-element Mass Fractions in Novae from Optical and Ultraviolet Spectroscopy

Object	Year	Reference	H	He	C	N	O	Ne	Na-Fe	Z	$(Z/Z_{\odot})$	$(Ne/Ne_{\odot})$	CNO/Ne-Fe
Solar	...	1	0.71	0.27	0.0031	0.001	0.0097	0.0018	0.0034	0.019	1.0	1.0	2.7
T Aur	1891	2	0.47	0.40	...	0.079	0.051	...	...	0.13	6.8	...	...
RR Pic	1925	3	0.53	0.43	0.0039	0.022	0.0058	0.011	...	0.043	2.3	6.3	2.9
DQ Her	1934	4	0.34	0.095	0.045	0.23	0.29	...	...	0.57	30.	...	...
DQ Her	1934	5	0.27	0.16	0.058	0.29	0.22	...	...	0.57	30.	...	...
HR Del	1967	6	0.45	0.48	...	0.027	0.047	0.0030	...	0.077	4.1	1.7	25.
V1500 Cyg	1975	7	0.49	0.21	0.070	0.075	0.13	0.023	...	0.30	16.	13.	12.
V1500 Cyg	1975	8	0.57	0.27	0.058	0.041	0.050	0.0099	...	0.16	8.4	5.6	15.
V1668 Cyg	1978	9	0.45	0.23	0.047	0.14	0.13	0.0068	...	0.32	17.	3.9	47.
V1668 Cyg	1978	10	0.45	0.22	0.070	0.14	0.12	...	...	0.33	17.	...	...
V693 CrA	1981	11	0.40	0.21	0.004	0.069	0.067	0.023	...	0.39	21.	128.	...
V693 CrA	1981	12	0.29	0.32	0.046	0.080	0.12	0.17	0.016	0.39	21.	97.	1.3
V693 CrA	1981	10	0.16	0.18	0.0078	0.14	0.21	0.26	0.030	0.66	35.	148.	1.2
V1370 Aql	1982	13	0.053	0.088	0.035	0.14	0.051	0.52	0.11	0.86	45.	296.	0.36
V1370 Aql	1982	10	0.044	0.10	0.050	0.19	0.037	0.56	0.017	0.86	45.	296.	0.48
GQ Mus	1983	14	0.37	0.39	0.0081	0.13	0.095	0.0023	0.0039	0.2 4	13.	1.2	38.
PW Vul	1984	15	0.69	0.25	0.0033	0.049	0.014	0.00066	...	0.067	3.5	0.38	100.
PW Vul	1984	10	0.47	0.23	0.073	0.14	0.083	0.0040	0.0048	0.30	16.	2.3	34.
PW Vul	1984	16	0.617	0.247	0.018	0.069	0.0443	0.001	0.0027	0.14	7.7	1.	31.
QU Vul	1984	17	0.30	0.60	0.0013	0.018	0.039	0.040	0.0049	0.10	5.3	23.	1.3
QU Vul	1984	10	0.33	0.26	0.0095	0.074	0.17	0.086	0.063	0.40	21.	49.	1.7
QU Vul	1984	18	0.36	0.19	...	0.071	0.19	0.18	0.0014	0.44	23.	100.	1.4
V842 Cen	1986	10	0.41	0.23	0.12	0.21	0.030	0.00090	0.0038	0.36	19.	0.51	77.
V827 Her	1987	10	0.36	0.29	0.087	0.24	0.016	0.00066	0.0021	0.35	18.	0.38	124.
QV Vul	1987	10	0.68	0.27	...	0.010	0.041	0.00099	0.00096	0.053	2.8	0.56	26.
V2214 Oph	1988	10	0.34	0.26	...	0.31	0.060	0.017	0.015	0.40	21.	9.7	12.
V977 Sco	1989	10	0.51	0.39	...	0.042	0.030	0.026	0.0027	0.10	5.3	15.	2.5
V433 Sct	1989	10	0.49	0.45	...	0.053	0.0070	0.00014	0.0017	0.062	3.3	0.80	33.
V351 Pup	1991	19	0.37	0.25	0.0056	0.076	0.19	0.11	...	0.38	20.	63.	2.4
V1974 Cyg	1992	18	0.19	0.32	...	0.085	0.29	0.11	0.0051	0.49	27.	68.	3.2
V1974 Cyg	1992	20	0.30	0.52	0.015	0.023	0.10	0.037	0.075	0.18	9.7	21.	3.1
V838 Her	1991	11	0.60	0.31	0.012	0.012	0.004	0.056	...	0.09	0.11	31.	...

Gehrz et al 1998, PASP

Abundance determinations from IR observations

Gehrz et al 1998, PASP

Nova	X	Y	$\frac{(n_X/n_Y)_{nova}}{(n_X/n_Y)_\odot}$
QU Vul/1984 #2	Ne	H	≥1.2
QU Vul/1984 #2	Al	Si	70
QU Vul/1984 #2	Mg	Si	4.7
QU Vul/1984 #2	Ne	Si	≥6.4
V1974 Cyg/1992	Ne	H	≥4
V1974 Cyg/1992	Ne	H	≥10
V1974 Cyg/1992	Ne	Si	≈35
V1974 Cyg/1992	Al	Si	≈5
V1974 Cyg/1992	Mg	Si	≥3
V1974 Cyg/1992	C	H	≈12
V1974 Cyg/1992	N	H	≈50
V1974 Cyg/1992	O	H	≈25
V1974 Cyg/1992	Ne	H	≈50
V1974 Cyg/1992	Mg	H	≈5
V1974 Cyg/1992	Al	H	≈5
V1974 Cyg/1992	Si	H	≈6
V1974 Cyg/1992	S	H	≈5
V1974 Cyg/1992	Ar	H	≈5
V1974 Cyg/1992	Fe	H	≈4
V1974 Cyg/1992	Ne	O	≈4
V705 Cas/1993	Silicates	H	≈15
V705 Cas/1993	C	H	≈45
Nova Aql/1995	C	H	≤0.6

Nova Models: need of core-envelope mixing

- Z observed >> solar → mixing CO or ONe core – solar envelope accreted
- Explosion itself (fast nova) → initial overabundance of CNO → mixing

Nova Models: need of core-envelope mixing

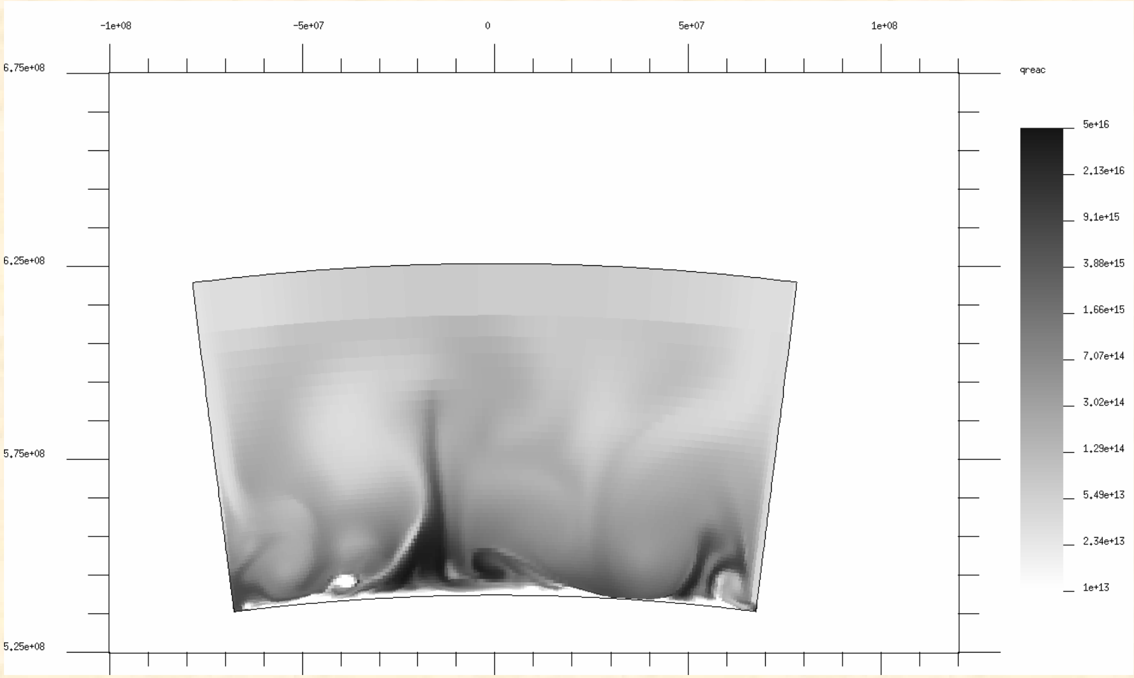

Logarithm of the burning rates close to the peak of the runaway

Glasner et al. 1997

Glasner & Livne 2002

Shear instabilities of the transversal component of the convective flow induce mixing of CNO elements from the core.

Convective cells and convective velocities are bigger than those predicted by the 1D MLT.

Nova Models: need of core-envelope mixing

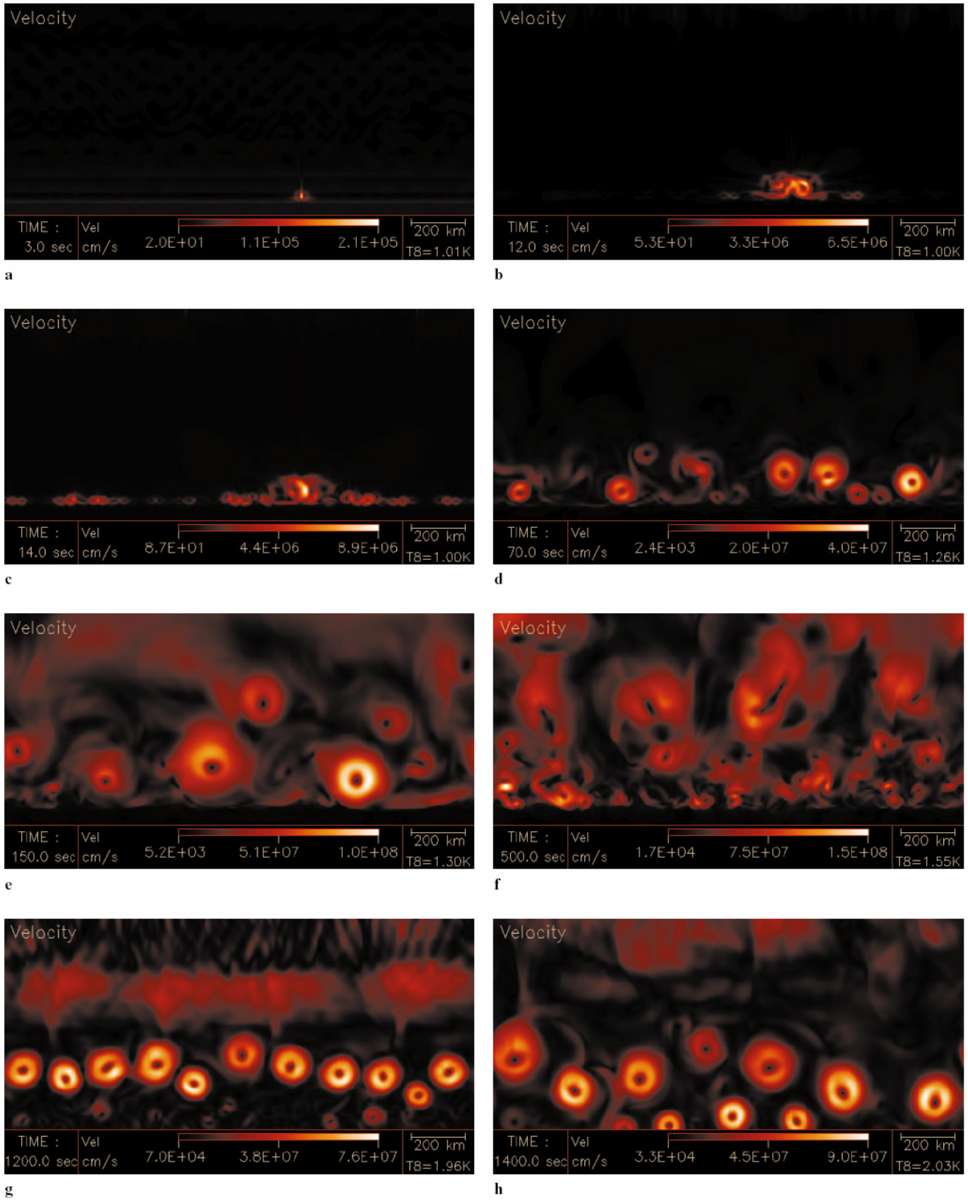

Fig. 1a–h. Velocity field at different stages of the evolution for the low resolution run. The color coding is done according to the absolute value of the velocity at each point. T8 denotes the temperature of the hottest individual zone.

Flow dominated by small convective eddies

More limited dredge-up and mixing

Kercek et al. 1998, A&A

The Sensitivity of Multidimensional Nova Calculations to the outer Boundary Condition

Glasner, Livne & Truran, 2005

In this study, we demonstrate that the imposed outer boundary condition can have a dramatic effect on the solution. Several commonly used choices for the outer boundary conditions are examined. It is shown that the solutions obtained from Lagrangian simulations, where the envelope is allowed to expand and mass is being conserved, are consistent with spherically symmetric solutions. In Eulerian schemes which utilize an outer boundary condition of free outflow, the outburst can be artificially quenched.

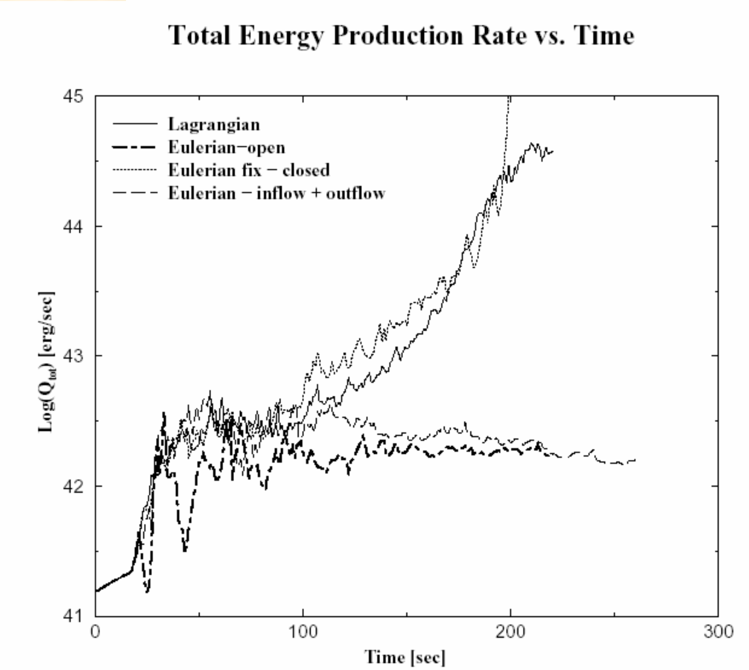

Nuclear energy

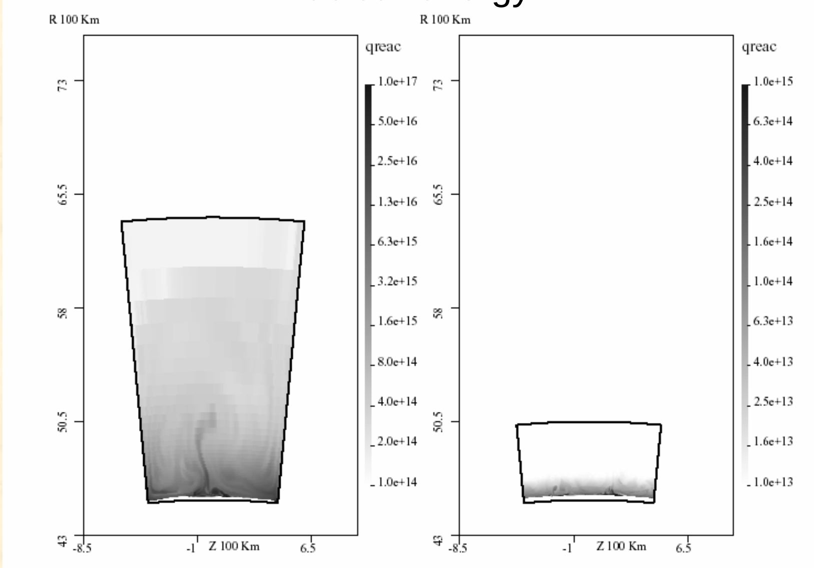

Lagrangian

Pure Eulerian

ON HEAVY ELEMENT ENRICHMENT IN CLASSICAL NOVAE

A. Alexakis,[1,2] A. C. Calder,[1,3] A. Heger,[1,4,5] E. F. Brown,[1,3] L. J. Dursi,[1,3] J. W. Truran,[1,3,4] R. Rosner,[1,2,3,4] D. Q. Lamb,[1,3,4] F. X. Timmes,[1,3] B. Fryxell,[1,4] M. Zingale,[6] P. M. Ricker,[7,8] and K. Olson[1,9]

ApJ, 602 (2004)

Many classical nova ejecta are enriched in CNO and Ne. Rosner and coworkers recently suggested that the enrichment might originate in the resonant interaction between large-scale shear flows in the accreted H/He envelope and gravity waves at the interface between the envelope and the underlying C/O white dwarf. The shear flow amplifies the waves, which eventually form cusps and break. This wave breaking injects a spray of C/O into the superincumbent H/He.

In the absence of enrichment prior to ignition, the base of the convective zone, does not reach the C/O interface. As a result, there is no additional mixing, and the runaway is slow. In contrast, the formation of a mixed layer during the accretion of H/He, prior to ignition, causes a more violent runaway. The envelope can be enriched by $\leq$ 25% of C/O by mass (consistent with that observed in some ejecta) for shear velocities, over the surface, with Mach numbers $\leq$ 0.4.

ON HEAVY ELEMENT ENRICHMENT IN CLASSICAL NOVAE

A. Alexakis,[1,2] A. C. Calder,[1,3] A. Heger,[1,4,5] E. F. Brown,[1,3] L. J. Dursi,[1,3] J. W. Truran,[1,3,4] R. Rosner,[1,2,3,4] D. Q. Lamb,[1,3,4] F. X. Timmes,[1,3] B. Fryxell,[1,4] M. Zingale,[6] P. M. Ricker,[7,8] and K. Olson[1,9]

ApJ, 602 (2004)

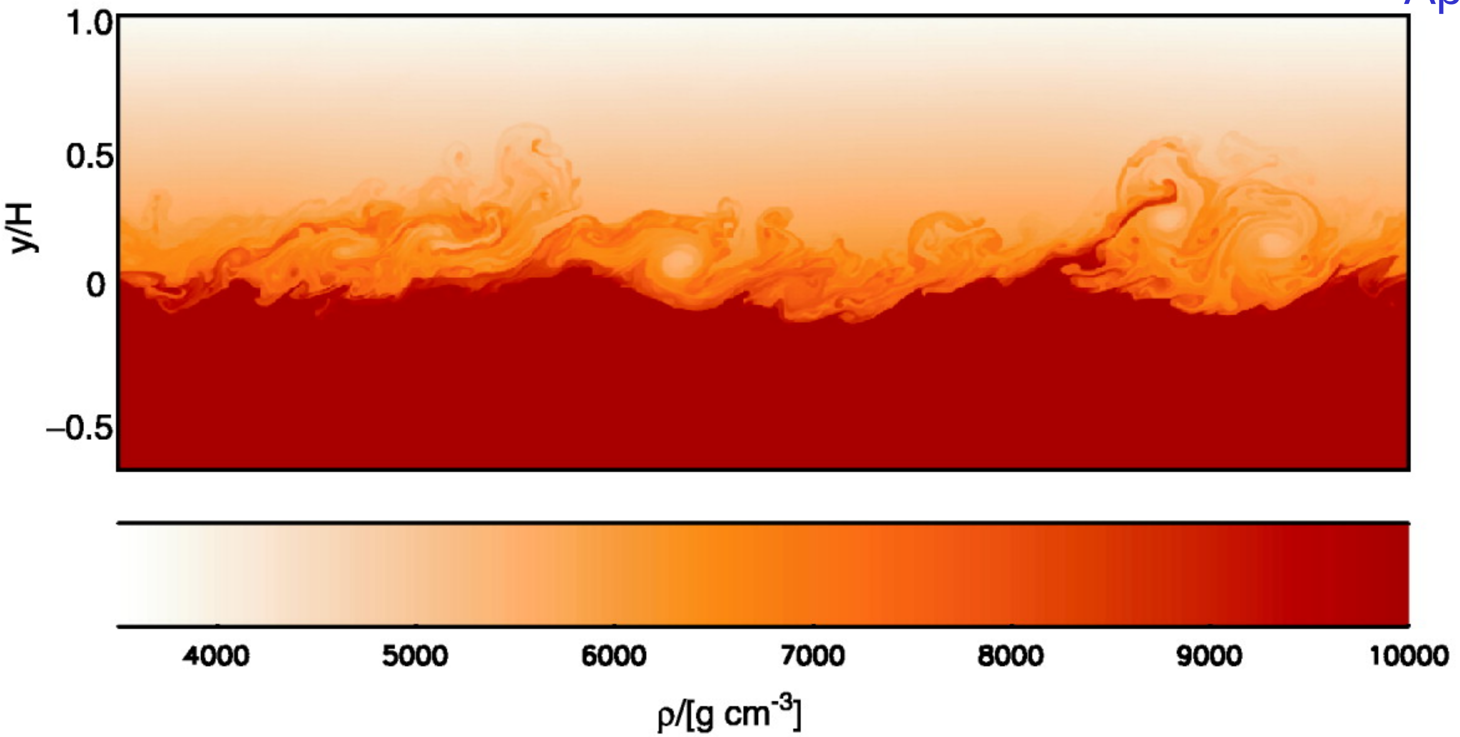

Fig. 1.—Breaking C/O waves, as determined by simulations in two dimensions. Gravity points toward the bottom of the figure, with the vertical distance y in units of the pressure scale height H, as evaluated just above the interface. The color scale indicates the mass density in units of g cm^{-3}.

Alexakis et al., ApJ, 602 (2004)

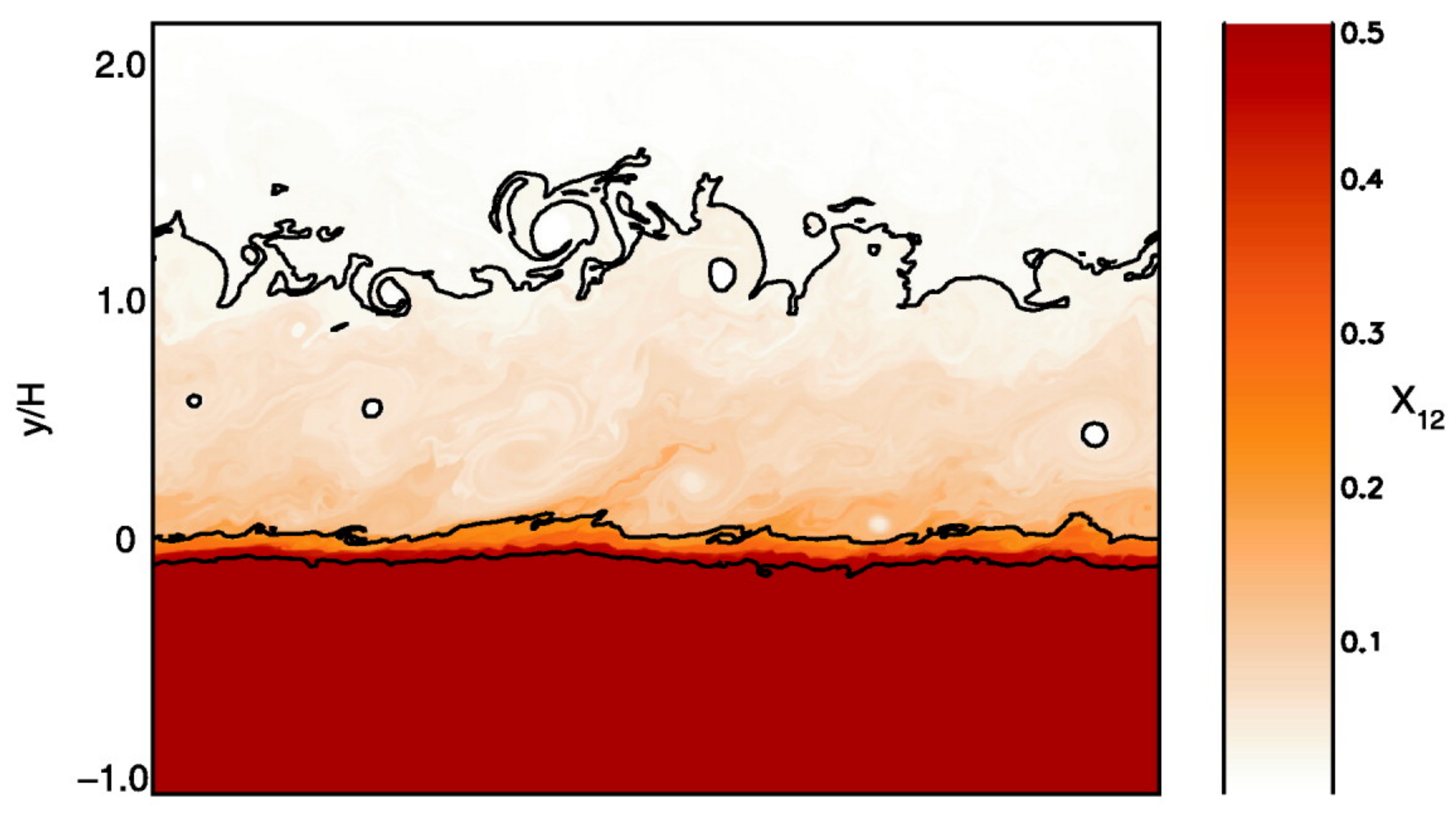

FIG. 2.—Mass fraction of ^{12}C for $\delta/H = 0.04$ after $t = 3500\delta/U$. The vertical dimension is scaled to the pressure scale height H as evaluated just above the interface. The contours for ^{12}C mass fractions are, from top to bottom, 0.02, 0.20, and 0.49.

Alexakis et al., ApJ, 602 (2004)

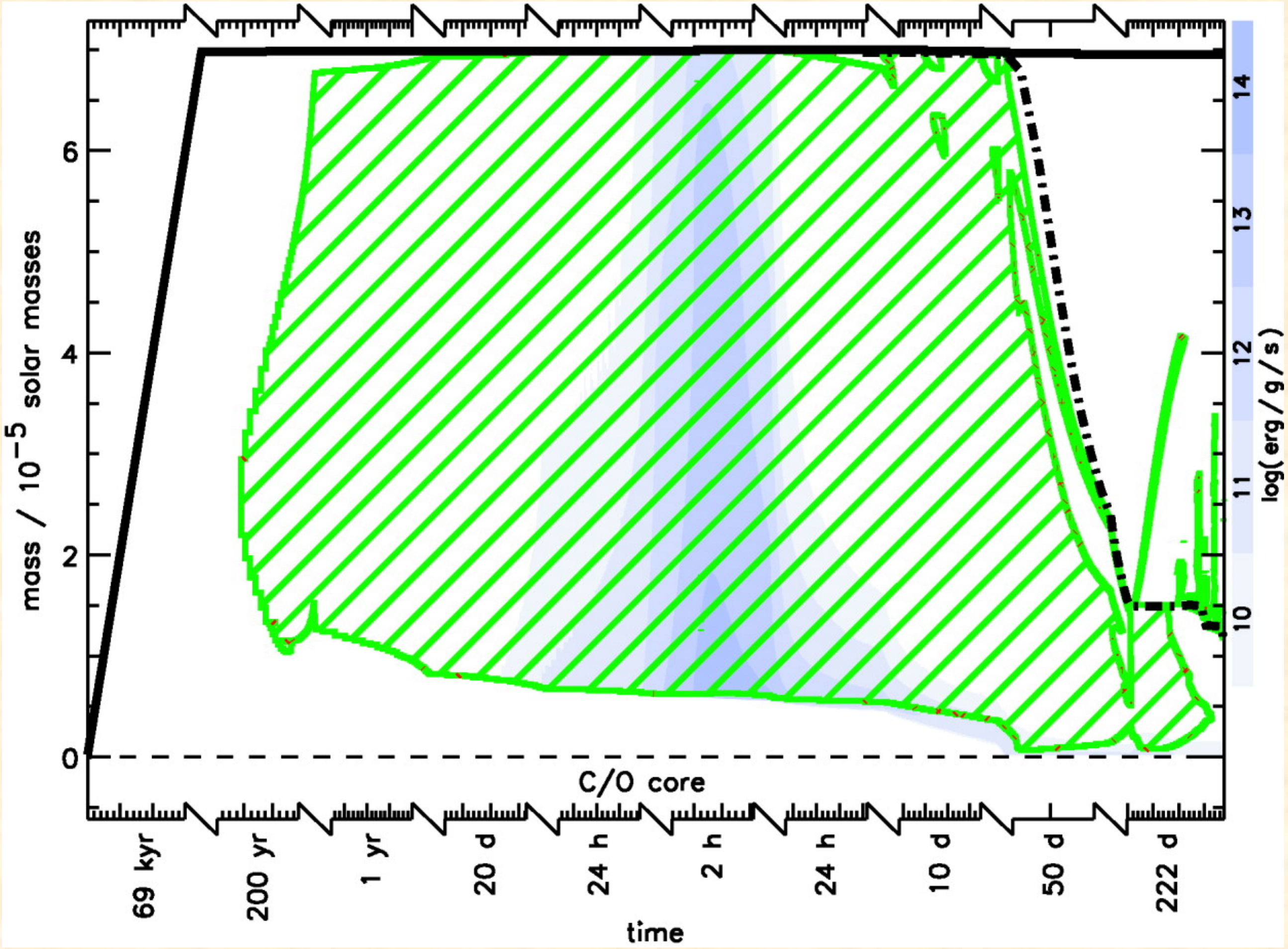

FIG. 4.—Kippenhahn diagram of a nova without enrichment. The *x*-axis indicates time intervals for the different evolution stages, and the *y*-axis gives the mass above the C/O WD substrate. Green hatching (framed by a green line) indicates convection, blue shading indicates nuclear energy generation, for which each level of darker blue denotes an increase by 1 order of magnitude, starting at 10^{10} ergs g^{-1} s^{-1}. The thick black line shows the total mass of the star (including ejecta), increasing through accretion; the dash-dotted line indicates the mass outside of 10^{12} cm; and the dashed line marks the interface between the C/O WD substrate and the accreted layers.

The underlying white dwarf

White dwarfs are the endpoints of the stellar evolution of stars with masses below 11-12 $M_\odot$.

- $M \leq$ 8-10 $M_\odot \rightarrow$ CO white dwarfs (He burning)
- 8-10 $M_\odot \leq M \leq 12\ M_\odot \rightarrow$ ONe white dwarfs (C burning)

10 $M_\odot \rightarrow$ 1.2 $M_\odot$ ONe core

The underlying white dwarf

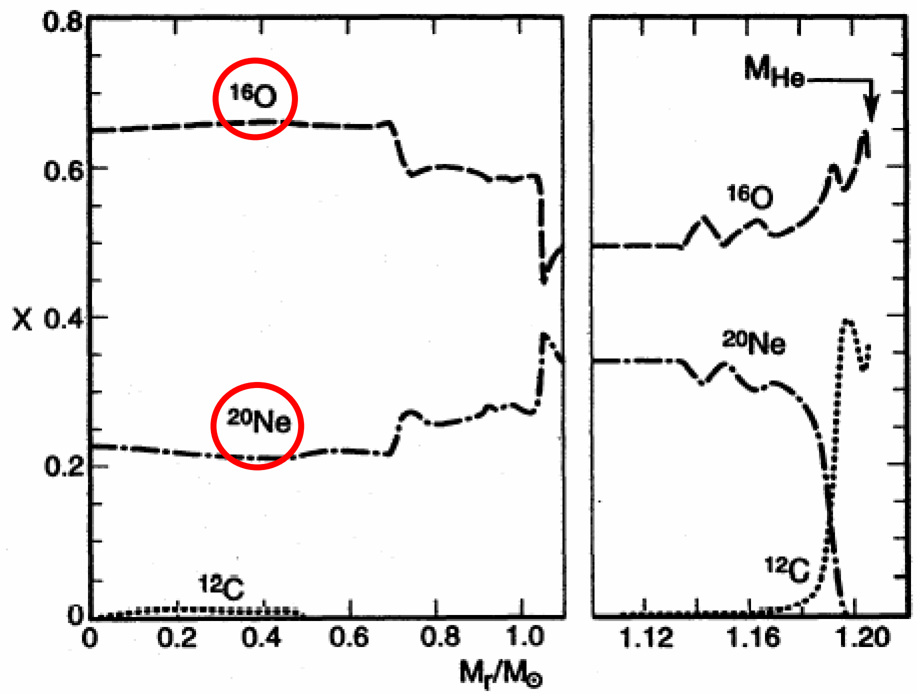

FIG. 7.—Abundances by mass of the major isotopes in the helium-exhausted interior at the end of the carbon-burning phase ($t = 7.1895212 \times 10^{14}$ s).

$10M_\odot$ mass Population I star evolved from the H-burning main sequence through carbon burning

↓

$1.2M_\odot$ ***ONe*** core

≠

ONeMg core predicted by hydrostatic C-burning (Arnett & Truran, 1969)

Ritossa, García-Berro & Iben, 1996, ApJ

see also Domínguez, Tornambè & Isern 1993

The underlying white dwarf

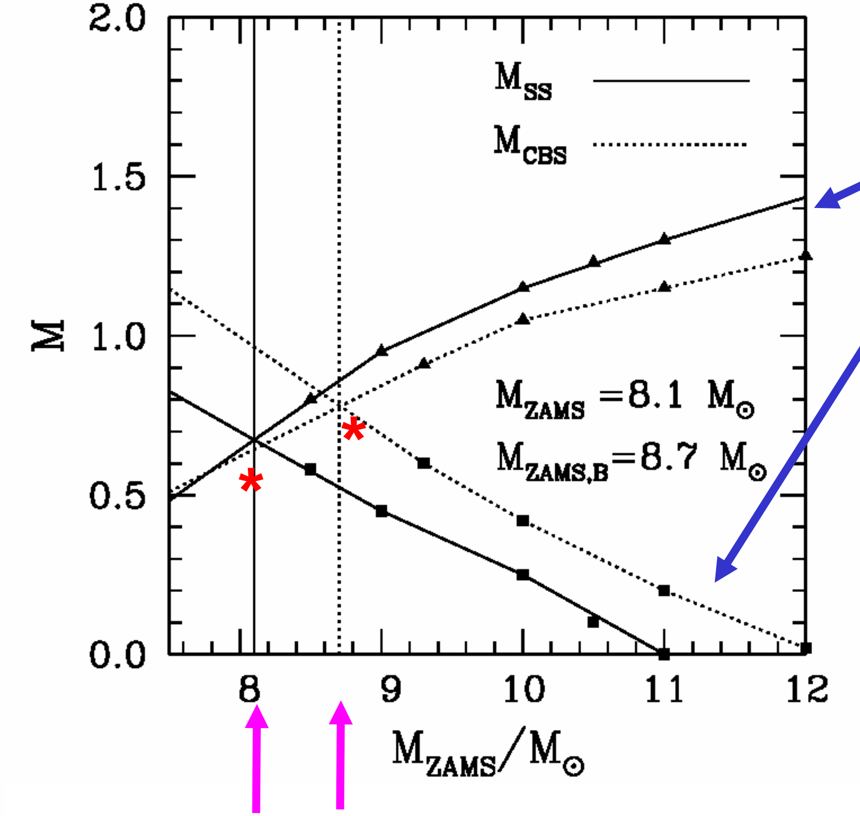

Gil Pons, García-Berro, José, Hernanz & Truran, 2003, A&A

Size of the CO core at the beginning of C burning, for single and binary evolution

Mass point at which C is ignited

Minimum mass required for C-ignition to take place (*): 8.1 $M_\odot$ (single) and 8.7 $M_\odot$ (binary)

Off-center C-ignition

Central C ignition:

11 $M_\odot$ for single evolution

12 $M_\odot$ for binary evolution

The underlying white dwarf

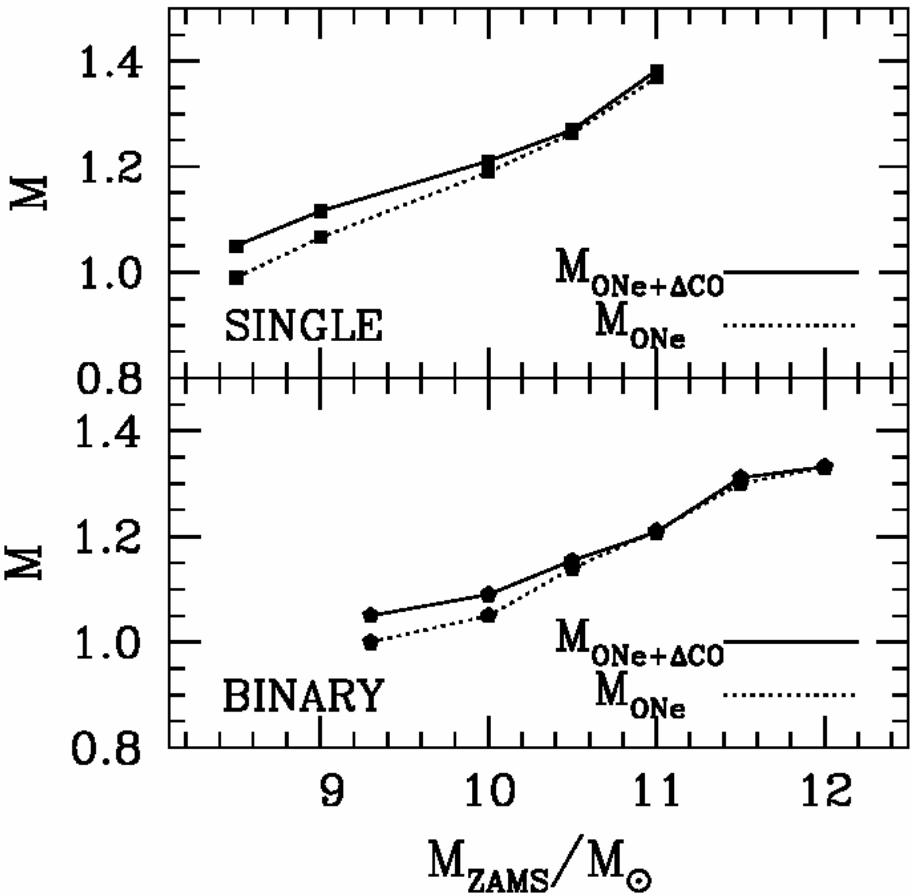

'ig. 3. Size of the final cores as a function of the ZAMS mass for ingle and binary star evolution.

ONe core mass with a “CO buffer” (binary evolution)

M_{ZAMS}	M_{ONe}	$M_{ONe+\Delta CO}$
9.3	1.00	1.07
10.0	1.05	1.09
10.5	1.14	1.15
11.0	1.21	1.22
11.5	1.30	1.31
12.0	1.33	1.33

Gil-Pons, García-Berro, José, Hernanz, Truran, 2003, A&A

Size of the final core for single and binary evolution: relevance of new $M_{initial}$-M_{final} mass relation for the fraction of novae hosting ONe white dwarfs: smaller number but still around 30%

The underlying White Dwarf

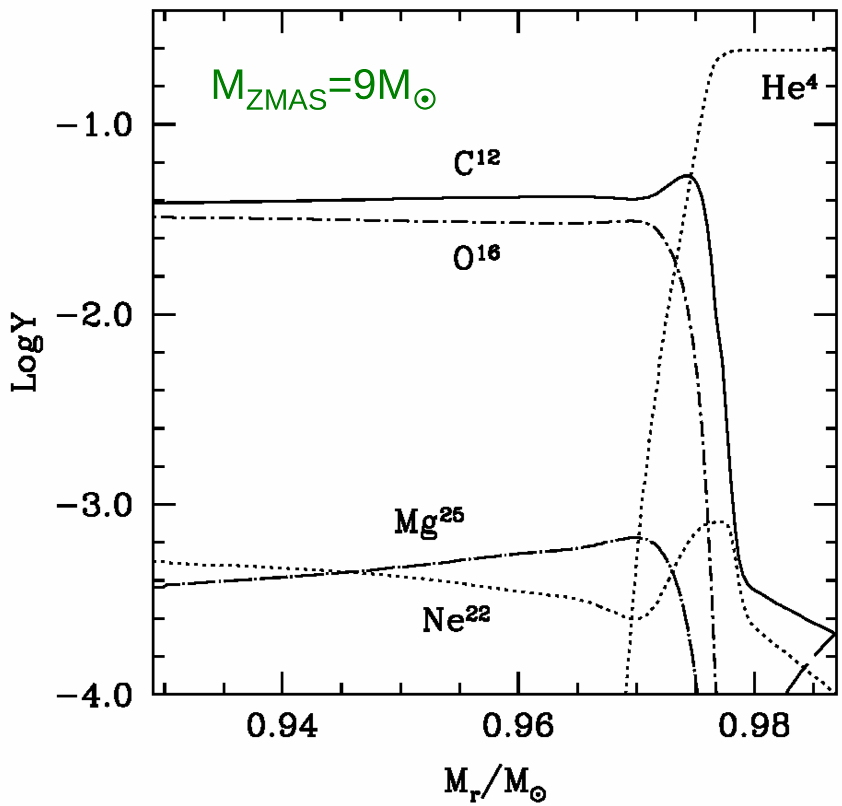

Fig. 6. Number abundances of the CO core resulting from 9 $M_\odot$ ZAMS primary component in a CBS.

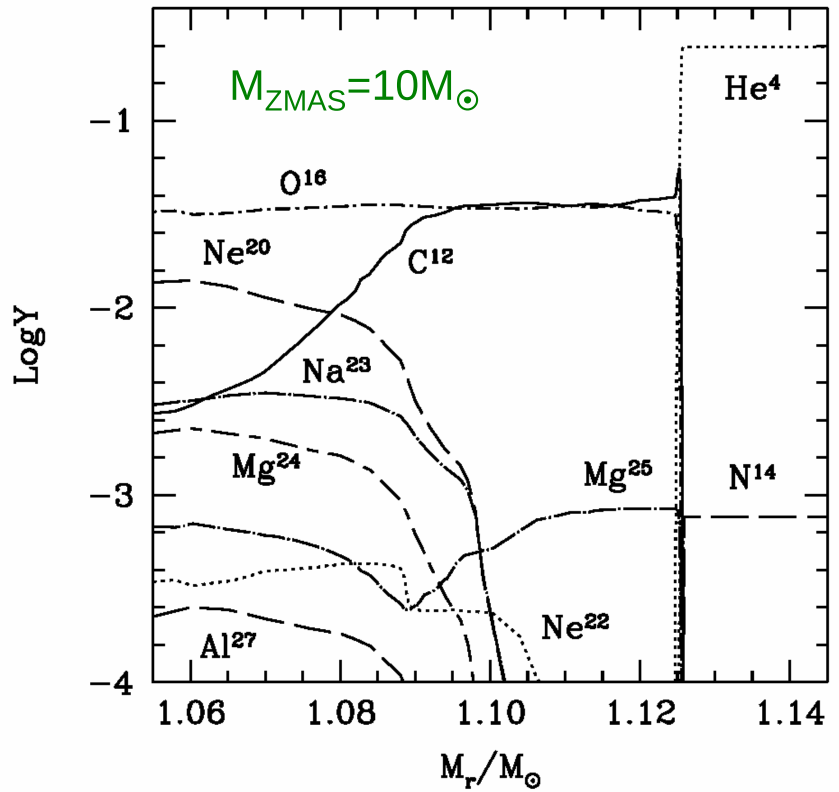

Fig. 5. Number abundances of the uppermost regions of an ONe white dwarf resulting from the evolution of a 10 $M_\odot$ ZAMS primary component in a close binary system.

"CO buffer" on top of an ONe core

(Gil-Pons et al., 2003, A&A)

The underlying White Dwarf

CO buffer on top of ONe core: weird nuclesoynthesis potentially leading to missclassification of novae

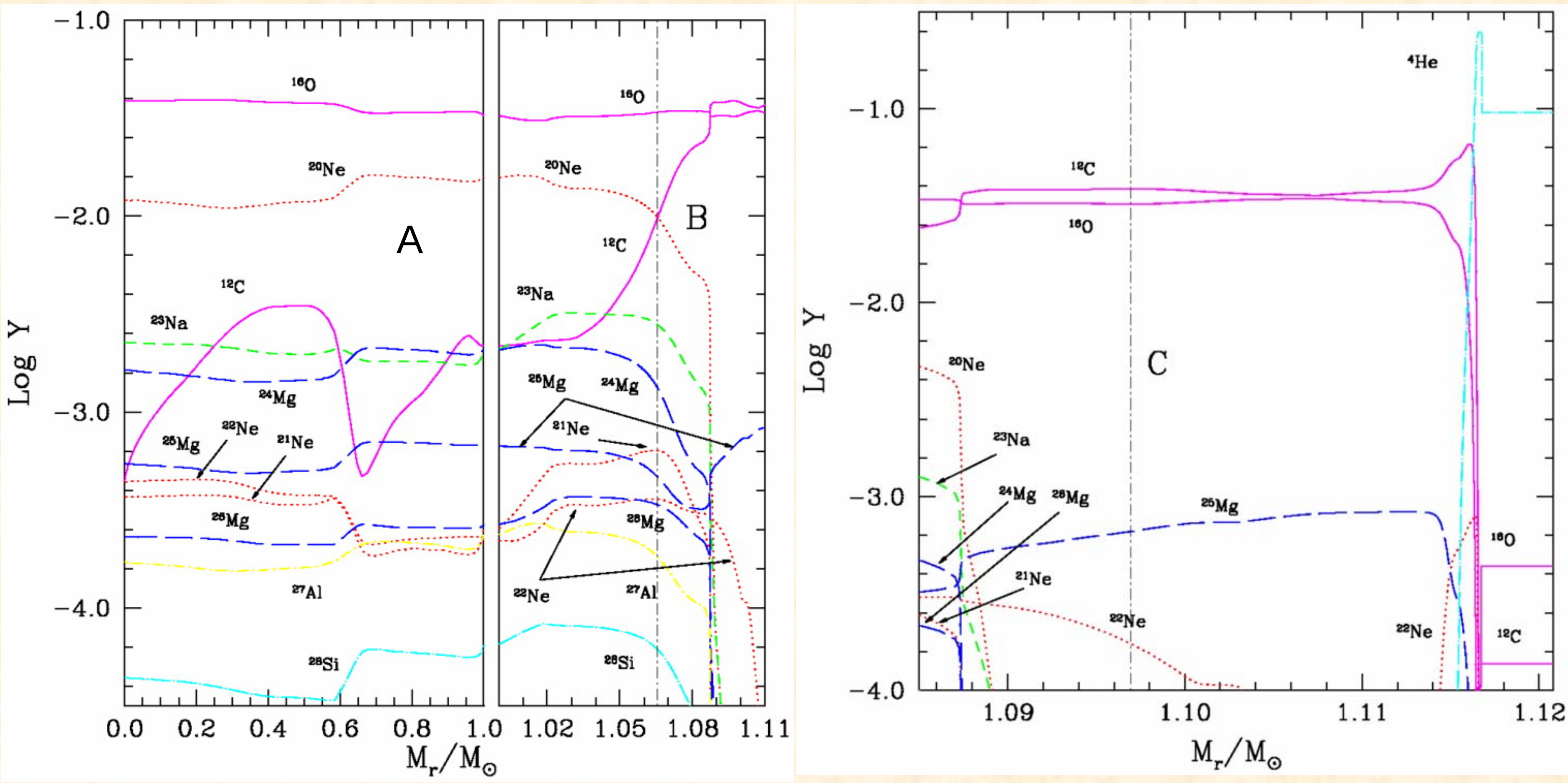

José, Hernanz, García-Berro, Gil-Pons, 2003, ApJL

The underlying White Dwarf

Relevance of CO buffer on top of ONe WD for nova nucleosynthesis: lack of Ne in the ejecta: misclassification of novae (non-Ne nova ≠ CO nova)

TABLE 1

RESULTS OF THE EVOLUTION OF 1.25 $M_\odot$ ONe WHITE DWARFS

Parameter	A	B	C
$X(^{12}C)_{initial}$	6.1 (−3)	6.0 (−2)	0.23
$X(^{16}O)_{initial}$	0.26	0.28	0.26
$X(^{20}Ne)_{initial}$	0.16	0.10	8.1 (−4)
ΔM_{env} (10^{-5} $M_\odot$)	2.20	1.54	1.23
t_{rise} (10^5 s)	121	33.7	2.54
t_{max} (s)	313	134	45
T_{peak} (10^8 K)	2.51	2.31	2.22
K_{ejec} (10^{45} ergs s^{-1})	1.52	1.13	1.04
ΔM_{ejec} (10^{-5} $M_\odot$)	1.79	1.25	1.00
$X(^1H)$	0.28	0.29	0.29
$X(^4He)$	0.22	0.21	0.18
$X(^7Li)$	7.7 (−7)	8.4 (−6)	1.1 (−5)
$X(^{12}C)$	2.4 (−2)	3.0 (−2)	4.7 (−2)
$X(^{13}C)$	3.3 (−2)	4.1 (−2)	7.3 (−2)
$X(^{14}N)$	3.9 (−2)	3.9 (−2)	1.1 (−1)
$X(^{15}N)$	4.3 (−2)	5.2 (−2)	6.8 (−2)
$X(^{16}O)$	6.8 (−2)	1.3 (−1)	1.9 (−1)
$X(^{17}O)$	5.5 (−5)	5.5 (−5)	5.5 (−5)
$X(^{18}F)$[a]	2.8 (−4)	3.4 (−4)	3.0 (−4)
$X(^{20}Ne)$	1.7 (−1)	1.2 (−1)	9.4 (−4)
$X(^{22}Na)$	3.3 (−4)	2.2 (−4)	9.3 (−7)
$X(^{26}Al)$	6.0 (−4)	6.0 (−4)	3.7 (−4)
$X(^{28}Si)$	5.8 (−2)	4.4 (−2)	6.6 (−3)
$X(^{29}Si)$	1.1 (−3)	4.8 (−4)	4.4 (−5)
$X(^{30}Si)$	6.3 (−3)	1.3 (−3)	4.7 (−5)

[a] The mass fraction of the radioactive isotope ^{18}F is given at 40 minutes after T_{peak}.

José, Hernanz, García-Berro, Gil-Pons, 2003, ApJL

- Scenario of nova explosions: thermonuclear runaway – Mixing between core and envelope material
- Properties of the underlying white dwarf: CO and ONe
- Theoretical models: general predictions as compared with observations
- Relevance of nucleosynthesis in classical novae:
    - chemical evolution of the Galaxy
    - presolar meteoritic grains
    - gamma-ray emission

Nova models : general properties

Parameter	CO1	CO2	CO3	CO4	CO5	CO6	CO7[a]
M_{wd} ($M_\odot$)	0.8	0.8	1.0	1.15	1.15	1.15	1.15
Mixing (%)	25	50	50	25	50	75	50
ΔM_{env} (10^{-5} $M_\odot$)	9.7	8.8	3.9	2.1	1.8	1.8	0.9
t_{acc} (10^5 yr)	3.1	2.6	1.7	1.2	1.0	1.0	0.4
t_{rise} (10^6 s)	2.8	1.8	1.1	0.43	0.72	0.48	1.7
$\epsilon_{nuc,max}$ (10^{16} ergs g^{-1} s^{-1})	0.05	0.1	0.3	0.5	1.1	1.9	0.2
T_{max} (10^8 K)	1.45	1.51	1.70	2.03	2.05	2.08	1.73
t_{max} (s)	454	199	152	147	65	51	200
ΔM_{ejec} (10^{-5} $M_\odot$)	7.0	6.4	2.3	1.5	1.3	1.3	0.63
v_{ejec} (km s^{-1})	800	1200	1900	2200	2700	2900	2700
K (10^{45} ergs)	0.6	1.1	0.9	0.8	1.0	1.3	0.45

José & Hernanz, 1998, ApJ

Parameter	ONe1	ONe2	ONe3	ONe4	ONe5	ONe6	ONe7
M_{wd} ($M_\odot$)	1.00	1.15	1.15	1.15	1.25	1.35	1.35
Mixing (%)	50	25	50	75	50	50	75
ΔM_{env} (10^{-5} $M_\odot$)	6.4	3.2	3.2	3.5	2.2	0.54	0.58
t_{acc} (10^5 yr)	3.3	1.9	1.9	2.1	1.3	0.31	0.33
t_{rise} (10^6 s)	20	46	13	11	6.8	2.5	2.1
$\epsilon_{nuc,max}$ (10^{16} ergs g^{-1} s^{-1})	0.29	0.36	0.76	2.4	2.1	19	14
T_{max} (10^8 K)	1.98	2.21	2.19	2.48	2.44	3.24	3.32
t_{max} (s)	768	828	540	305	380	150	108
ΔM_{ejec} (10^{-5} $M_\odot$)	4.7	2.3	1.9	2.6	1.4	0.44	0.34
v_{ejec} (km s^{-1})	1600	2100	2400	2500	3100	4100	6000
K (10^{45} ergs)	1.3	1.1	1.2	1.9	1.4	0.9	1.3

José & Hernanz 1998

Nova models : general properties

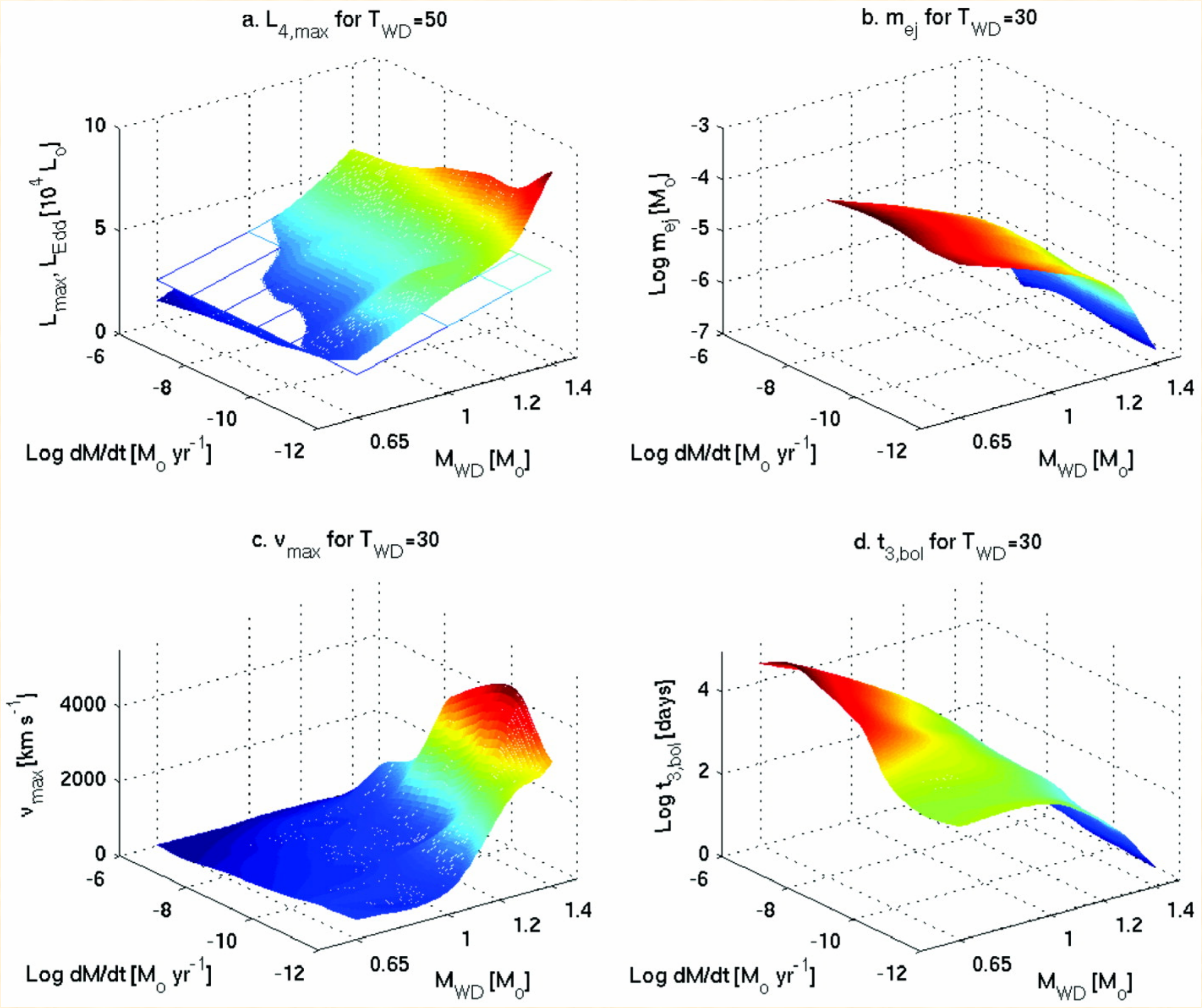

CO novae

Yaron, Prialnik, Shara & Kovetz, 2005

Ratio of ejected to accreted mass

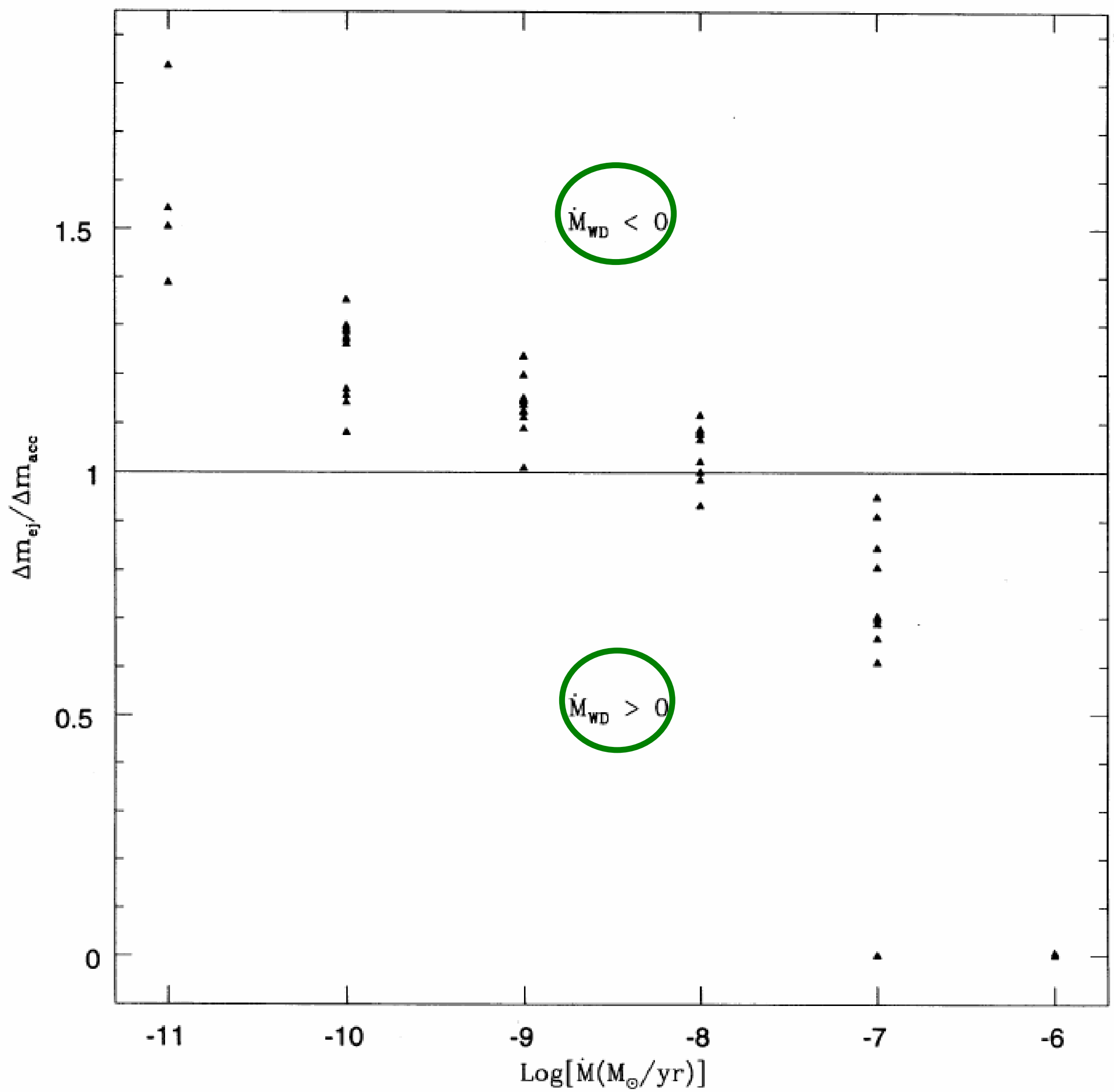

Prialnik & Kovetz, 1995

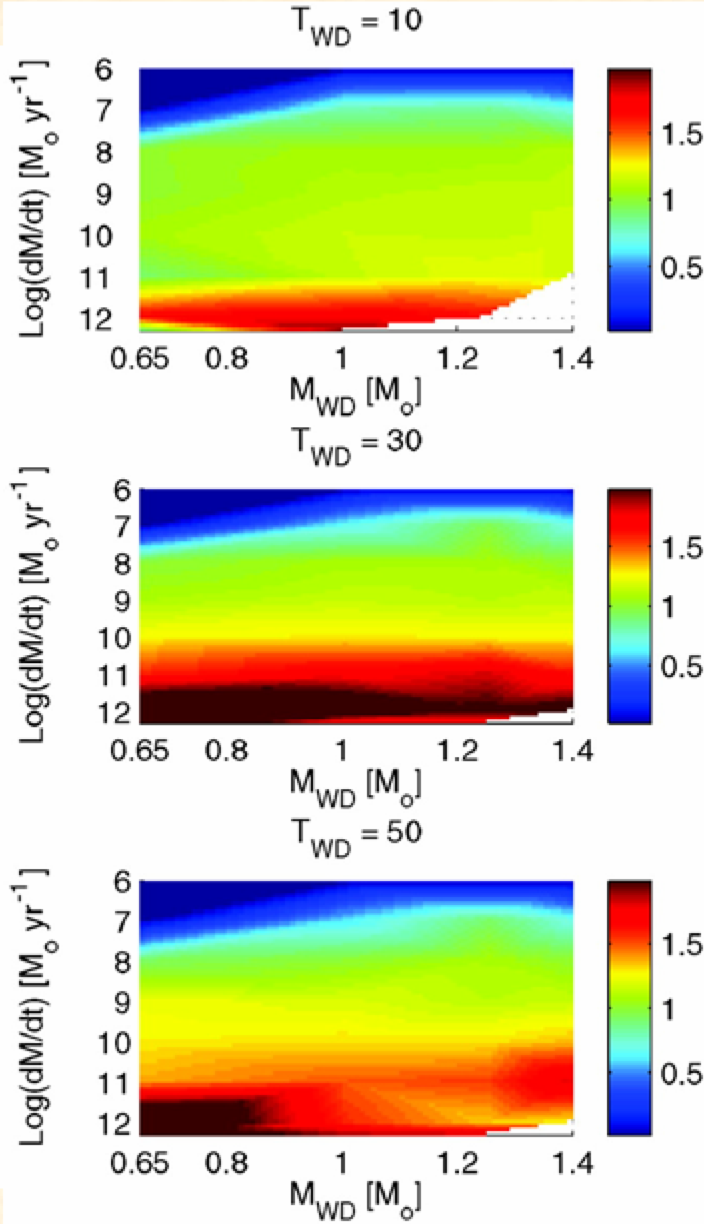

Yaron, Prialnik, Shara & Kovetz, 2005

Nova models: main nuclear reactions

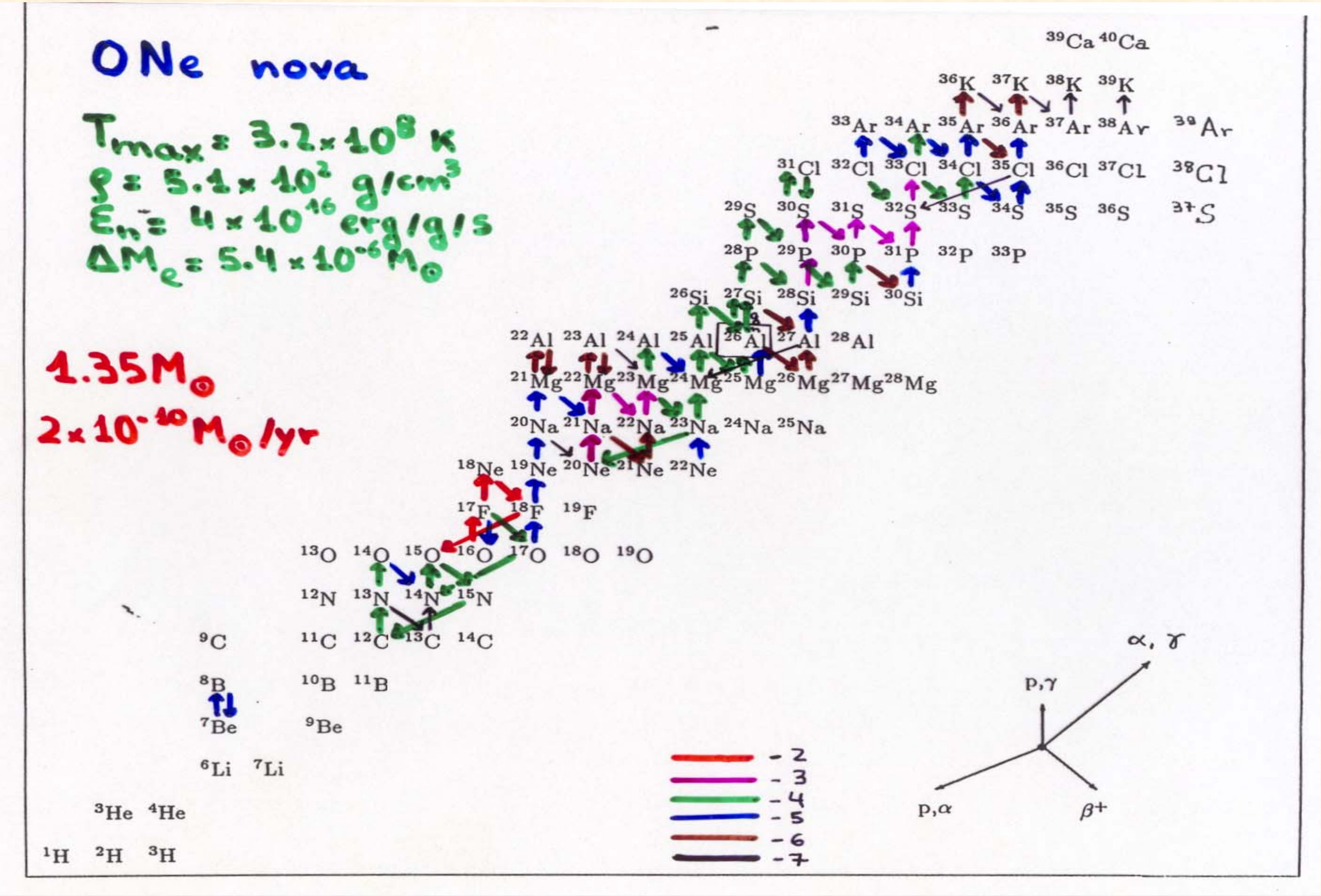

Models versus Observations of Some Classical Nova Systems

Model	H	He	C	N	O	Ne	Na–Fe	Z
V693 CrA 1981								
Vanlandingham et al. 1997	0.25	0.43	0.025	0.055	0.068	0.17	0.058	0.32
Model ONe3	0.30	0.20	0.051	0.045	0.15	0.18	0.065	0.50
Andreä et al. 1994	0.16	0.18	0.0078	0.14	0.21	0.26	0.030	0.66
Model ONe4	0.12	0.13	0.049	0.051	0.28	0.26	0.10	0.75
Williams et al. 1985	0.29	0.32	0.0046	0.080	0.12	0.17	0.016	0.39
Model ONe5	0.28	0.22	0.060	0.074	0.11	0.18	0.071	0.50
V1370 Aql 1982								
Andreä et al. 1994	0.044	0.10	0.050	0.19	0.037	0.56	0.017	0.86
Model ONe7	0.073	0.17	0.051	0.18	0.14	0.24	0.14	0.76
Snijders et al. 1987	0.053	0.088	0.035	0.14	0.051	0.52	0.11	0.86
Model ONe7	0.073	0.17	0.051	0.18	0.14	0.24	0.14	0.76
QU Vul 1984								
Austin et al. 1996	0.36	0.19	...	0.071	0.19	0.18	0.0014	0.44
Model ONe1	0.32	0.18	0.030	0.034	0.20	0.18	0.062	0.50
Saizar et al. 1992	0.30	0.60	0.0013	0.018	0.039	0.040	0.0049	0.10
Model ONe2	0.47	0.28	0.041	0.047	0.037	0.090	0.0035	0.25
PW Vul 1984								
Andreä et al. 1994	0.47	0.23	0.073	0.14	0.083	0.0040	0.0048	0.30
Model CO4	0.47	0.25	0.073	0.094	0.10	0.0036	0.0017	0.28
V1688 Cyg 1978								
Andreä et al. 1994	0.45	0.22	0.070	0.14	0.12	...	...	0.33
Model CO4	0.47	0.25	0.073	0.094	0.10	0.0036	0.0017	0.28
Stickland et al. 1981	0.45	0.23	0.047	0.14	0.13	0.0068	...	0.32
Model CO1...	0.51	0.21	0.048	0.096	0.13	0.0038	0.0015	0.28

José & Hernanz, 1998, ApJ

- Scenario of nova explosions: thermonuclear runaway – Mixing between core and envelope material
- Properties of the underlying white dwarf: CO and ONe
- Theoretical models: general predictions as compared with observations
- Relevance of nucleosynthesis in classical novae:
  - chemical evolution of the Galaxy
  - presolar meteoritic grains
  - gamma-ray emission

Nova Nucleosynthesis and chemical evolution of the Galaxy

M_{ejec}(theor.) ~ $2\times10^{-5}\ M_\odot$/nova

R(novae) ~ 35 novae/yr

Age of the Galaxy ~ 10^{10} yrs

$$M_{ejec,total}(\text{novae}) \sim 7\times10^{6}\ M_\odot = (7\times10^{-4}\ M_\odot/\text{yr}) \approx 1/3000\ M_{gal}(\text{gas+dust})$$

Novae can account for the galactic abundances of the isotopes they overproduce (w.r.t. sun) by factors ***≥ 3000***

Novae nucleosynthesis: overproductions w.r.t. solar

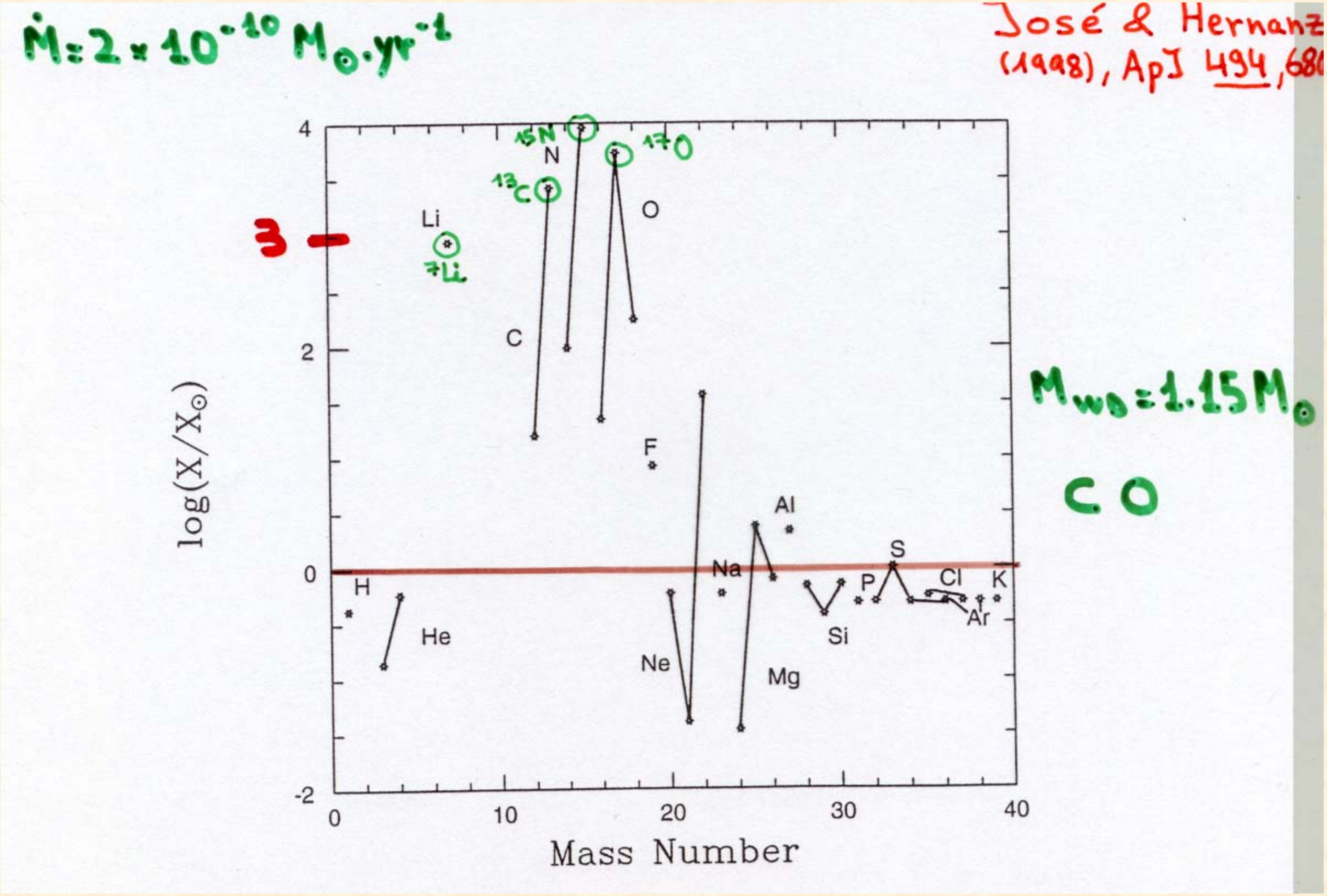

Novae nucleosynthesis: overproductions w.r.t. solar

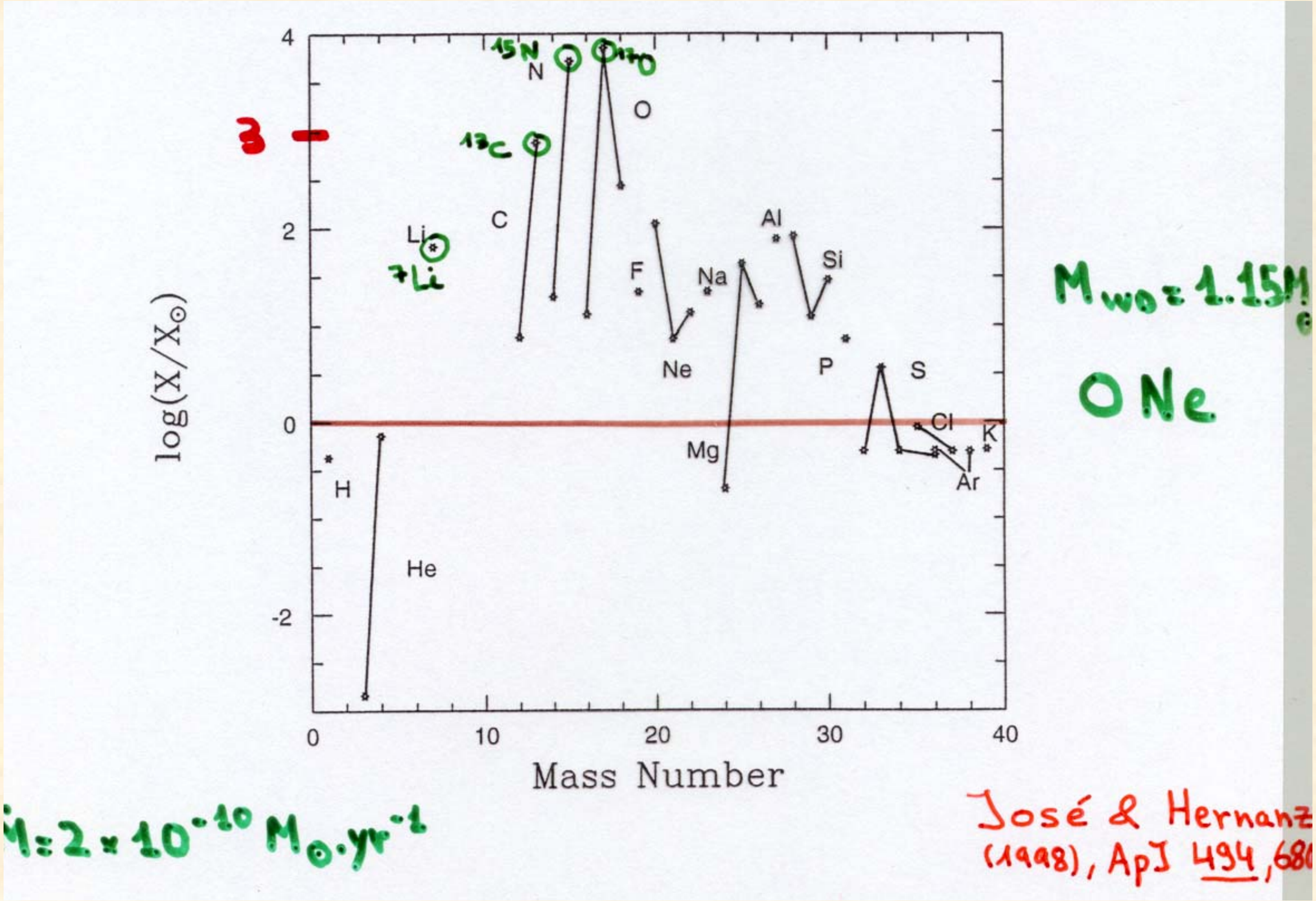

Novae nucleosynthesis: overproductions w.r.t. solar

ONe

1.35M$_\odot$

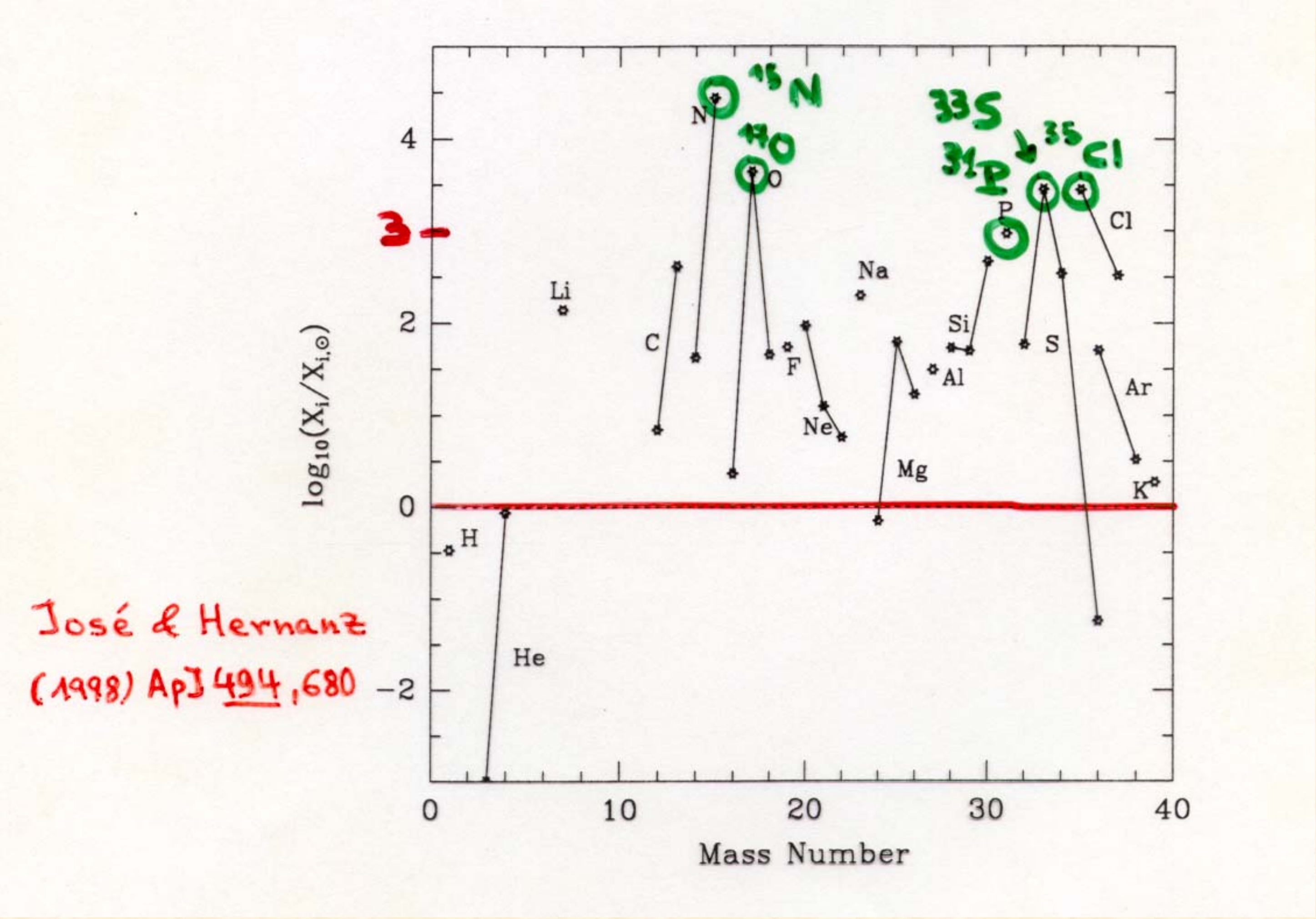

Nova nucleosynthesis and Galactic evolution of the CNO isotopes

MNRAS, 2004

Donatella Romano[1,2] and Francesca Matteucci[3]
[1]International School for Advanced Studies, SISSA/ISAS, Via Beirut 2-4, I-34014 Trieste, Italy
[2]INAF, Osservatorio Astronomico di Bologna, Via Ranzani 1, I-40127 Bologna, Italy; romano@bo.astro.it
[3]Dipartimento di Astronomia, Università di Trieste, Via G.B. Tiepolo 11, I-34131 Trieste, Italy; matteucci@ts.astro.it

In this paper, we adopt detailed nucleosynthesis in the ejecta of classical novae as published by José & Hernanz (1998) for a grid of hydrodynamical nova models spanning a wide range of CO and ONe WD masses ($0.8 - 1.35\ M_\odot$) and mixing levels between the accreted envelope and the outermost shells of the underlying WD core (25% – 75%). We find that, when included in a detailed model for the chemical evolution of the Milky Way, they produce $^{12}C/^{13}C$, $^{14}N/^{15}N$ and $^{16}O/^{17}O$ ratios decreasing with increasing metallicity, i.e., decreasing with time at the solar radius and increasing with Galactocentric distance at the present time, in agreement with the trends inferred from observations. However, if novae are

CNO: ^{13}C, ^{15}N, ^{17}O

Astron. Astrophys. 352, 117–128 (1999)

The galactic lithium evolution revisited*

D. Romano[1,2], F. Matteucci[3,1], P. Molaro[2], and P. Bonifacio[2]

[1] SISSA/ISAS, Via Beirut 2–4, 34014 Trieste, Italy
[2] Osservatorio Astronomico di Trieste, Via G.B. Tiepolo 11, 34131 Trieste, Italy
[3] Dipartimento di Astronomia, Università di Trieste, Via G.B. Tiepolo 11, 34131 Trieste, Italy

Received 26 April 1999 / Accepted 5 October 1999

In order to reproduce the upper envelope of the A(Li) vs [Fe/H] diagram we need to take into account several stellar Li sources: AGB stars, Type II SNe and novae. In particular, novae are required to reproduce the steep rise of A(Li) between the formation of the Solar System and the present time, as is evident from the data we sampled. On the other hand, ^{7}Li yields for SNeII should be lowered by at least a factor of two in order to reproduce the extension of the Spite plateau.

^{7}Li

- Scenario of nova explosions: thermonuclear runaway – Mixing between core and envelope material
- Properties of the underlying white dwarf: CO and ONe
- Theoretical models: general predictions as compared with observations
- Relevance of nucleosynthesis in classical novae:
  - chemical evolution of the Galaxy
  - presolar meteoritic grains
  - gamma-ray emission

Dust in novae

IR observations indicate that dust grains are formed in many novae

Nova Cyg 1978

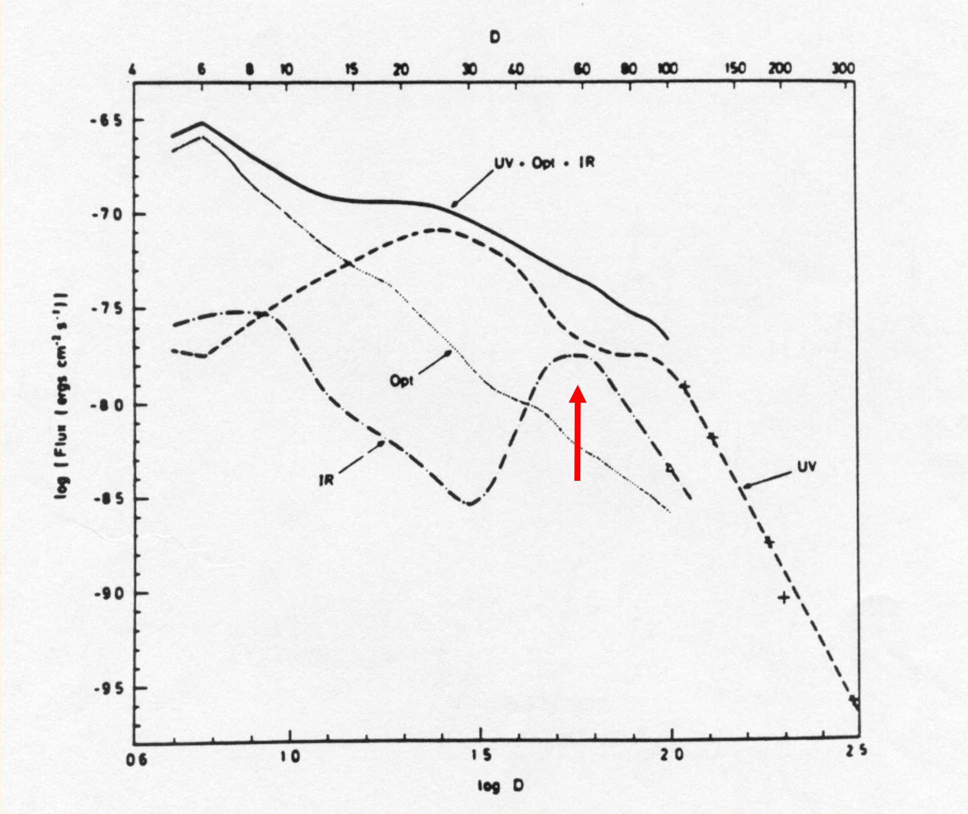

IR observations: dust formation

Nova	Year	V_o (km s^{-1})	Types of Dust Formed[b]	M_{gas} ($M_\odot$)	M_{dust} ($M_\odot$)
FH Ser	1970	560	C	...	...
V1229 Aql	1970	575	C	...	...
V1301 Aql	1975	...	C	...	...
V1500 Cyg[a]	1975	1180	...	$0.05–8 \times 10^{-4}$	...
NQ Vul	1976	750	C	10^{-4}	2×10^{-7}
V4021 Sgr	1977	...	C	...	...
LW Ser	1978	1250	C	2×10^{-5}	3.6×10^{-7}
V1668 Cyg	1978	1300	C	2×10^{-5}	2×10^{-8}
V1370 Aql[d]	1982	2800	C; SiC; SiO_2	...	...
GQ Mus	1983	600	No dust	$\leq 2.6 \times 10^{-6}$	...
PW Vul	1984 #1	285	C	$\leq 3.2 \times 10^{-6}$	5.1×10^{-10}
QU Vul[a]	1984 #2	1–5000	SiO_2	3×10^{-4}	10^{-8}
OS And[a,e]	1986	900	C?	...	...
V1819 Cyg[a]	1986	1000	No dust	...	...
V842 Cen	1986	1200	C; SiC; HC	...	...
V827 Her[a]	1987	1000	C	...	...
V4135 Sgr	1987	500	...	...	...
QV Vul	1987	700	C; SiO_2; HC; SiC	3×10^{-5}	3.4×10^{-8}
LMC 1988 #1	1988 #1	800	C?	...	...
LMC 1988 #2	1988 #2	1500	...	...	...
V2214 Oph	1988	500	...	...	...
V838 Her	1991	3500	C	$0.9–6.4 \times 10^{-4}$	3×10^{-5}
V1974 Cyg[a]	1992	2250	No dust	$2–5 \times 10^{-4}$	...
V705 Cas	1993	840	C; HC; SiO_2	$1–1.3 \times 10^{-5}$	2×10^{-6}
Aql 1995[a]	1995	1510	C	...	...

Novae and presolar meteoritic grains

Primitive meteorites contain presolar grains, which condensed in stellar atmospheres or in supernova or nova ejecta, and survived their "interstellar trip" and solar system formation

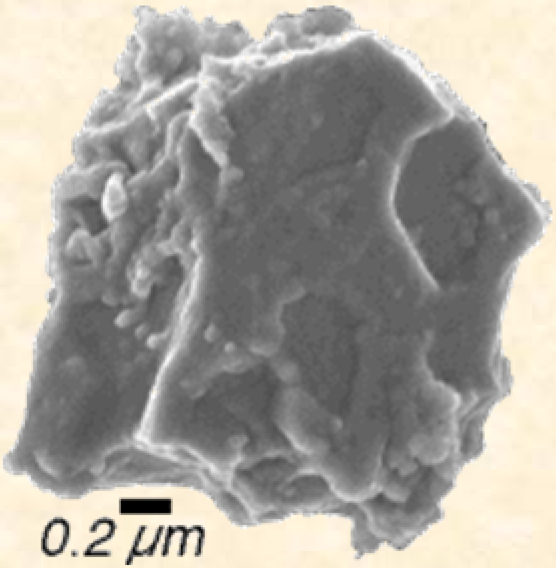

Isotopic abundances measurements in lab allow to ascertain their origin

Novae and presolar meteoritic grains

Five SiC and two graphite grains from the Murchison and Acfer 094 meteorites show isotopic compositions indicating a nova origin: Amari, Gao, Nittler, Zinner, José, Hernanz & Lewis (2001); José, Hernanz, Amari, Lodders & Zinner (2004)

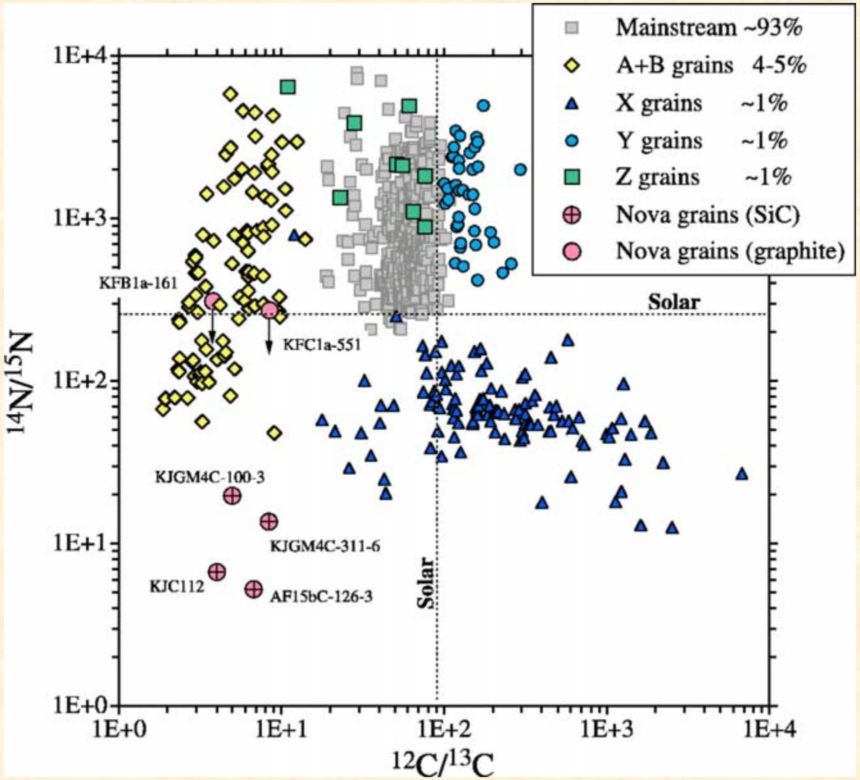

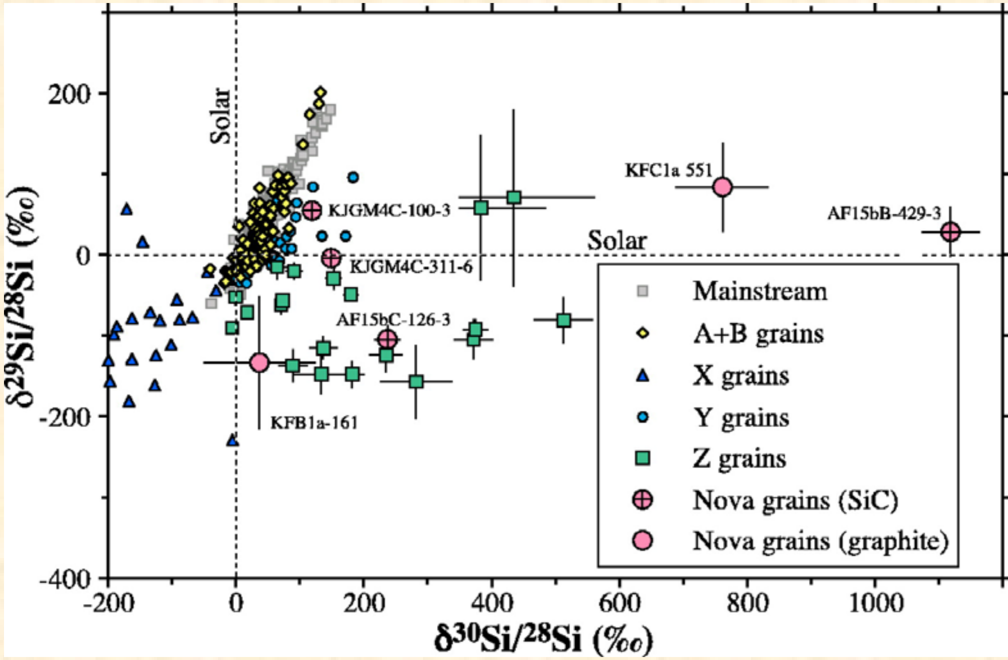

Novae and presolar meteoritic grains

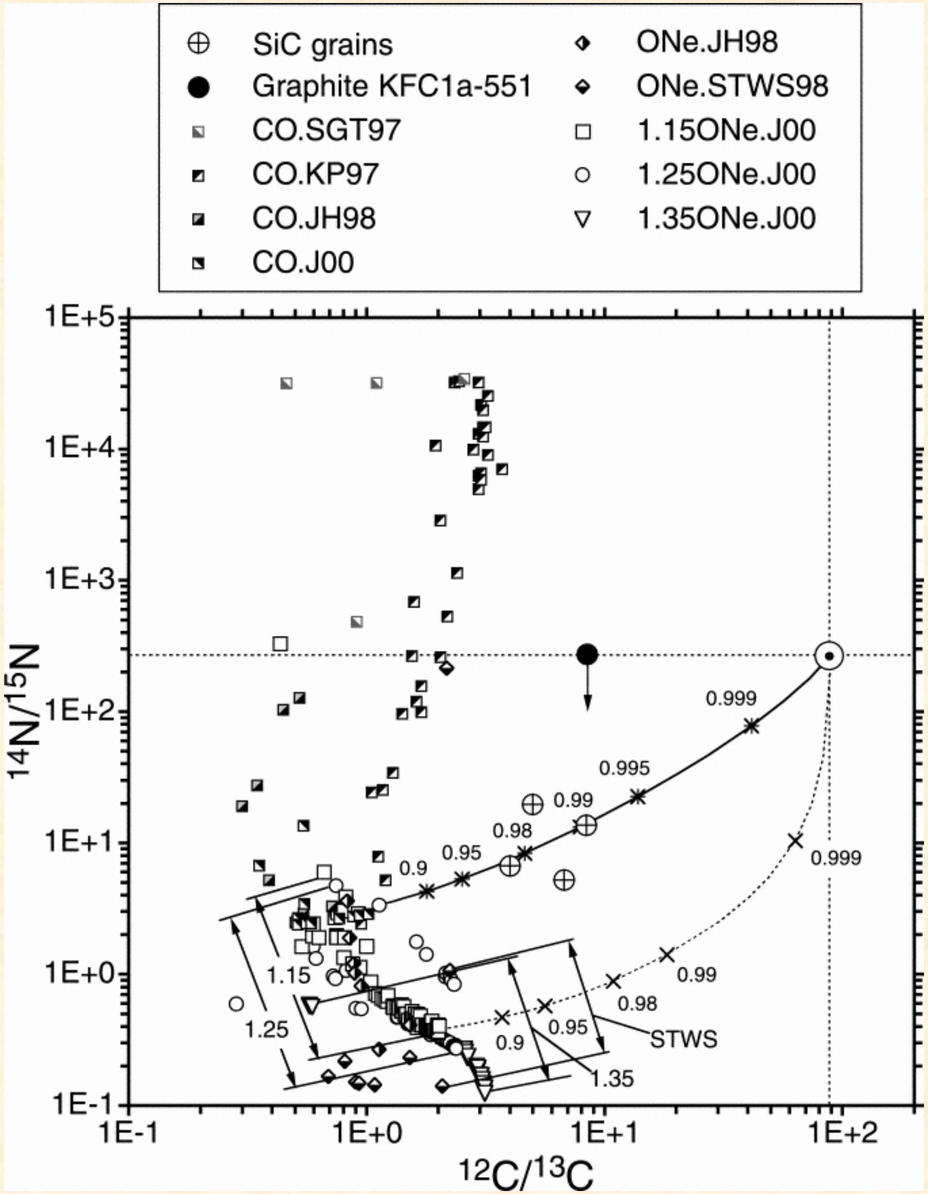

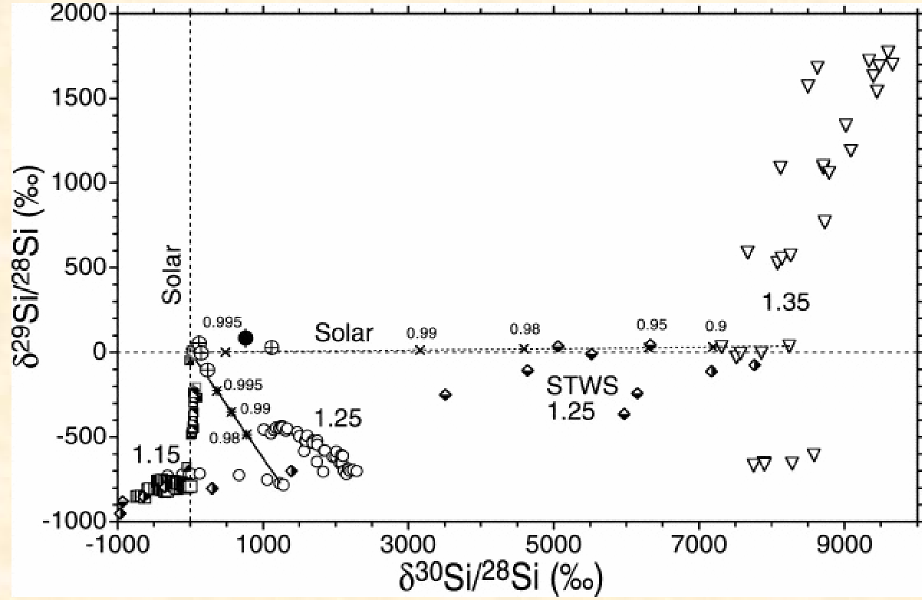

Amari et al. 2001

- Scenario of nova explosions: thermonuclear runaway – Mixing between core and envelope material
- Properties of the underlying white dwarf: CO and ONe
- Theoretical models: general predictions as compared with observations
- Relevance of nucleosynthesis in classical novae:
  - chemical evolution of the Galaxy
  - presolar meteoritic grains
  - gamma-ray emission

Why novae emit gamma-rays?

Explosive H-burning: synthesis of β^+-unstable nuclei

	^{13}N	^{14}O	^{15}O	^{17}F	^{18}F
τ	862s	102s	176s	93s	158min.

crucial for enve-
lope expansion

crucial for γ-ray emission
(through e^--e^+ annihilation)

Other radioactive nuclei synthesized

	^{7}Be	^{22}Na	^{26}Al
τ	77days	3.75yrs	10^6yrs
line	478keV	1275keV	1809keV
	e-capture	e^+-emission	e^+-emission

Main radioactive isotopes synthesized in classical novae

Nucleus	τ	Type of emission	Nova type
^{13}N	862 s	511 keV line continuum (E<511 keV)	CO and ONe
^{18}F	158 min	511 keV line continuum (E<511 keV)	CO and ONe
^{7}Be	77 days	478 keV line	CO mainly
^{22}Na	3.75 yr	1275 keV line	ONe
^{26}Al	1.0×10^{6} yr	1809 keV line	ONe

Spectra of CO novae

$M_{WD} = 1.15\ M_{\odot}$

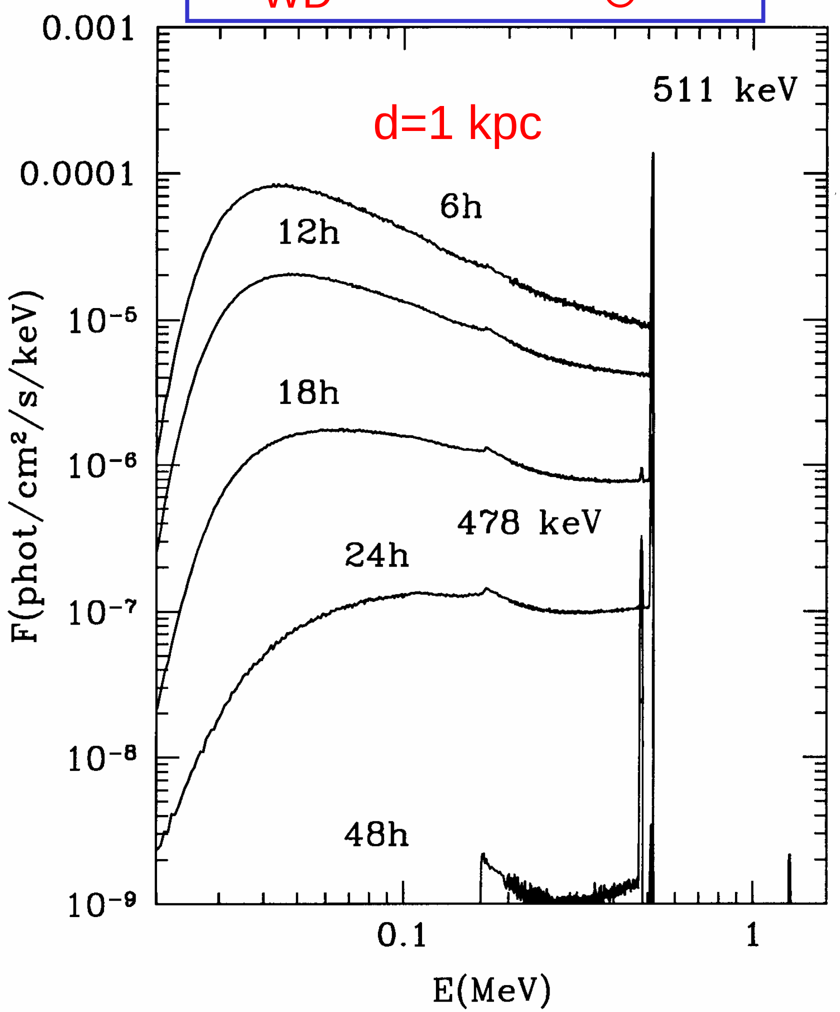

- e^+ annihilation and Comptonization ➡ continuum and 511 keV line; e^+ from ^{13}N and ^{18}F

➡ predicted theoretically by Clayton & Hoyle 1974; Leising & Clayton 1987

- photoelectric absorption ➡ cutoff at 20 keV
- 478 keV line from ^{7}Be decay
- transparent at 48 h

Gómez-Gomar, Hernanz, José, Isern,1998, MNRAS

Spectra of ONe novae

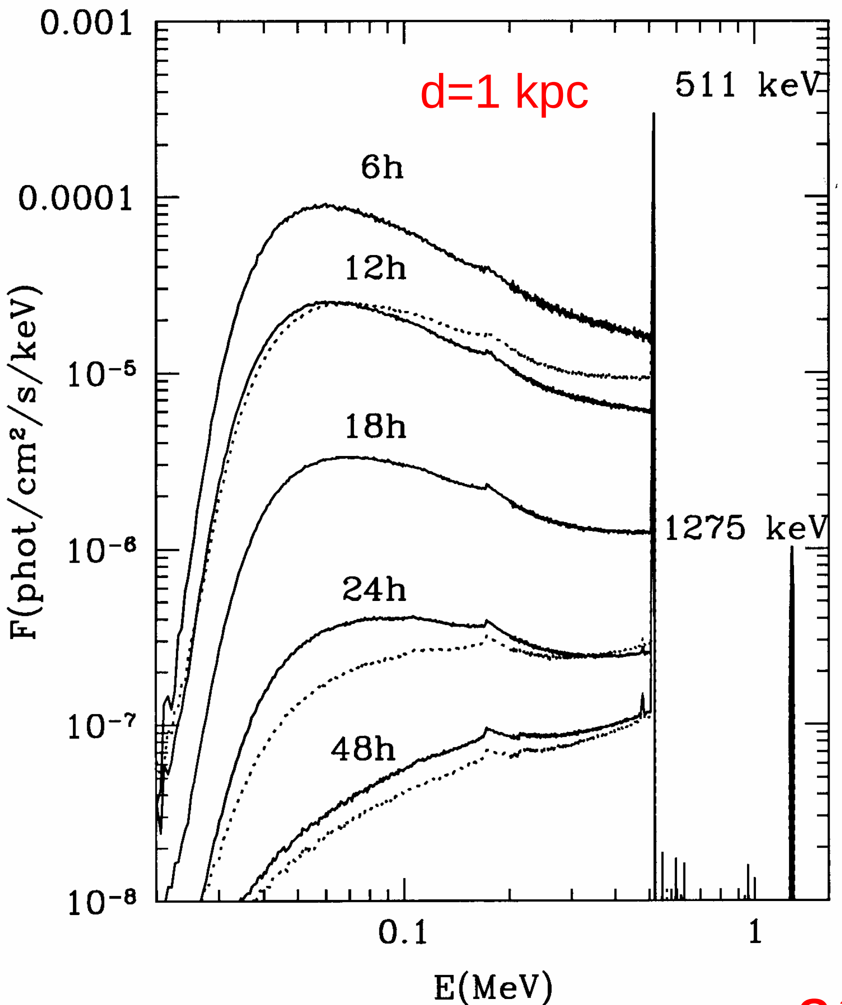

M_{WD} = 1.15 $M_\odot$ (solid)
1.25 $M_\odot$ (dotted)

- photoelectric absorption → cutoff at 30 keV
- continuum and 511 keV as in CO novae
- 1275 keV line from ^{22}Na decay
- similar behaviour for the 2 models, because of similar KE and yields

Gómez-Gomar, Hernanz, José, Isern,1998, MNRAS

Light curves: 1275 keV (^{22}Na) line

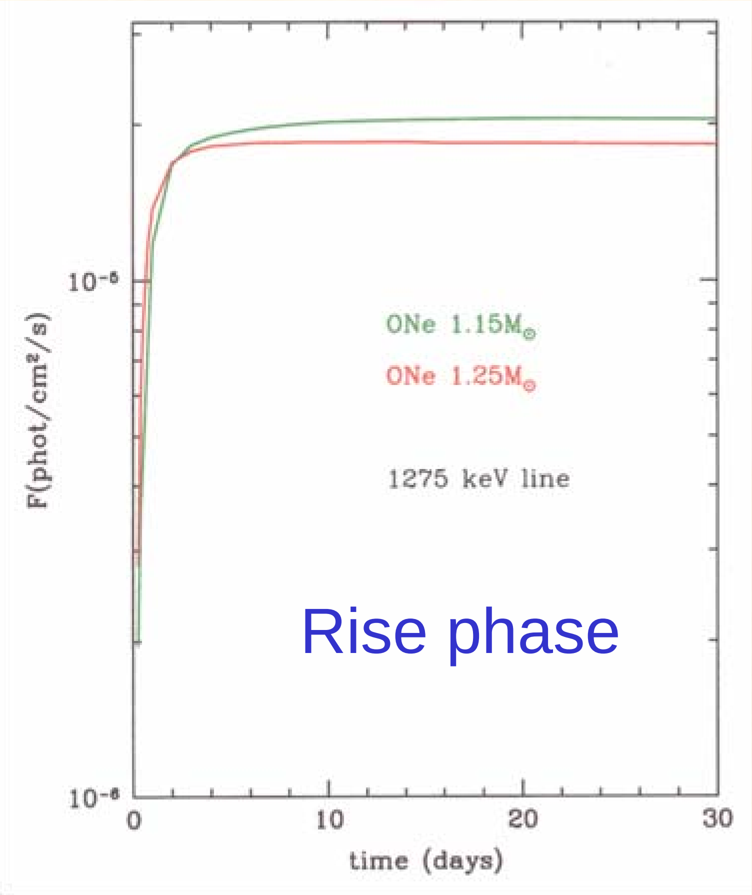

Only in ONe novae

d=1 kpc

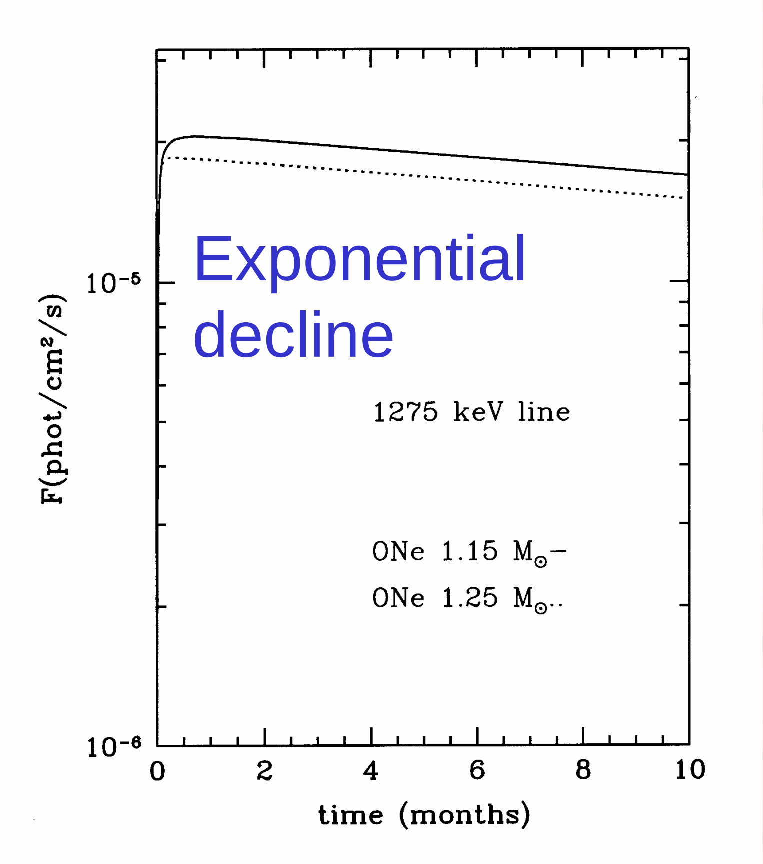

t_{max}: 20 days (1.15M$_\odot$),12 days (1.25 M$_\odot$), line width ~ 20 keV; duration: months

Flux (max) ~ 2x10^{-5} ph/cm^2/s; $M_{ejected}$(^{22}Na) ~ (6-7)x10^{-9}M$_\odot$

➡ predicted theoretically by Clayton & Hoyle, 1974

Light curves: 478 keV (^{7}Be) line

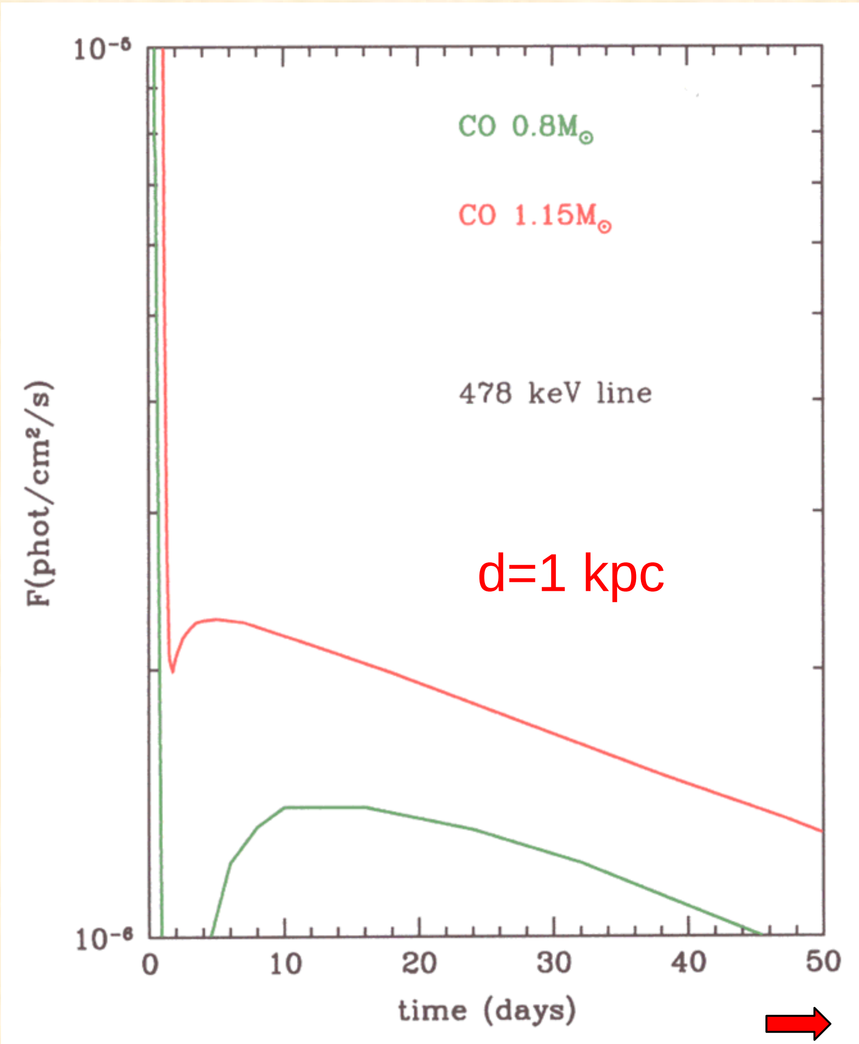

Only in CO novae

t_{max}: 13 days (0.8M$_\odot$)

5 days (1.15 M$_\odot$)

duration: some weeks

Flux ~ (1-2)x10^{-6} ph/cm^2/s

$M_{ejected}$(^{7}Be) ~ (0.7-1.1)x10^{-10}M$_\odot$

Line width: 3-7 keV

→ predicted theoretically by Clayton 1981

Prospects for detectability with INTEGRAL/SPI

*Table 1. SPI 3σ detectability of ^7Be (478 keV) and ^{22}Na (1275 keV) lines from classical novae**

Line (E Δ E,keV)	t_{obs}(ks)	F_{min} (ph/cm^2/s)	d(kpc)
478 (8)	10^3	7.98×10^{-5}	0.16
478 (8)	1.2×10^3	7.28×10^{-5}	0.17
478 (8)	2.4×10^3	5.15×10^{-5}	0.20
1275 (20)	10^3	7.28×10^{-5}	0.52
1275 (20)	1.2×10^3	6.64×10^{-5}	0.55
1275 (20)	2.4×10^3	4.70×10^{-5}	0.65

* F_{min} are the fluxes which would give a 3σ detection of the lines, with the quoted observation times, which have been computed with the Observation Time Estimator for INTEGRAL *OTE*. The detectability distances have been computed adopting as model fluxes for the 478 keV and 1275 keV lines, at 1 kpc, 2×10^{-6} and 2×10^{-5} ph/cm^2/s, for a typical CO and ONe nova, respectively (see Gómez-Gomar et al. (1998); Hernanz et al. (1999)).

Width of the lines fully taken into account

Future missions: MAX (γ-ray lens), ACT (Advanced Compton Telescope)

Light curves: 511 keV line

In CO and ONe novae

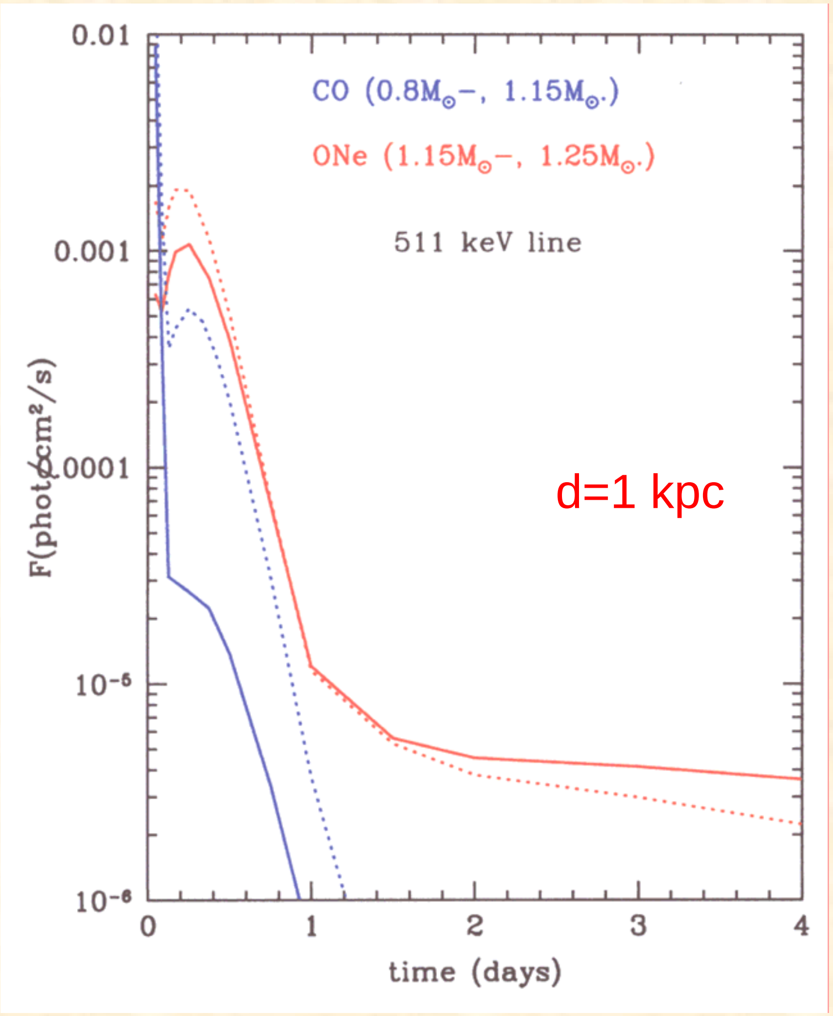

Model	t_{max}^* (h)	F_{max} ($ph/cm^2/s$)**
CO, 0.8 $M_\odot$	- - -	2.6×10^{-5}
CO, 1.15 $M_\odot$	6.5	5.3×10^{-4}
ONe, 1.15 $M_\odot$	6	1.0×10^{-3}
ONe, 1.25 $M_\odot$	5	1.9×10^{-3}

- 511 keV line in ONe novae remains after 2 days until ~ 1 week because of e^+ from ^{22}Na
- Intense (but short duration)
- Very early appearence, before visual maximum (i.e, before discovery)

Gamma-ray and visual light curves

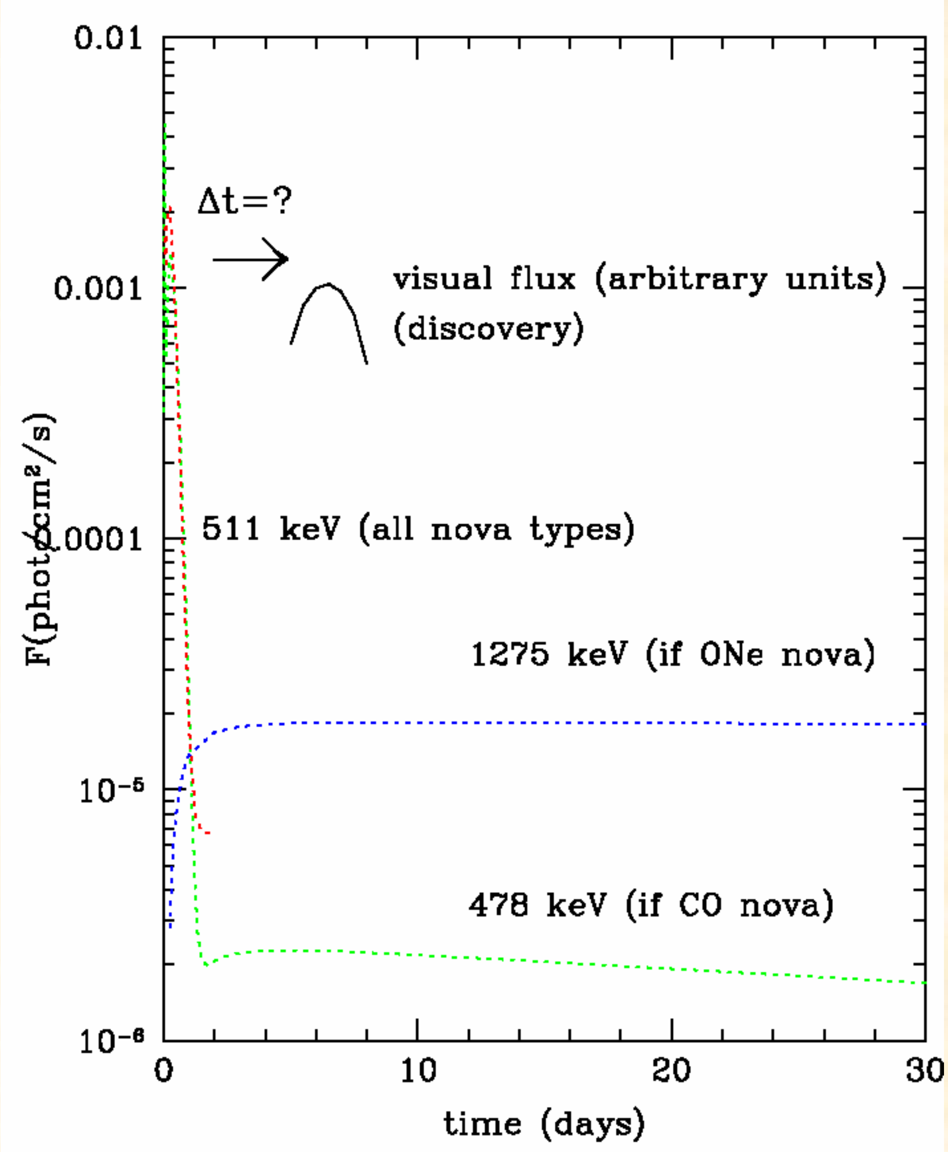

Visual maximum later than 511 keV and continuum maxima

The continuum and the 511 keV line, e^{-}-e^{+} annihilation, are the most intense γ-ray emissions, but their duration is very short and they appear before visual discovery

➡ detection requires “a posteriori” analyses with wide FOV instruments (BATSE, TGRS, RHESSI)

➡ future hard X/soft γ-ray surveys like EXIST can provide unique information about the Galactic nova distribution

Galactic distribution of γ-ray emission from novae

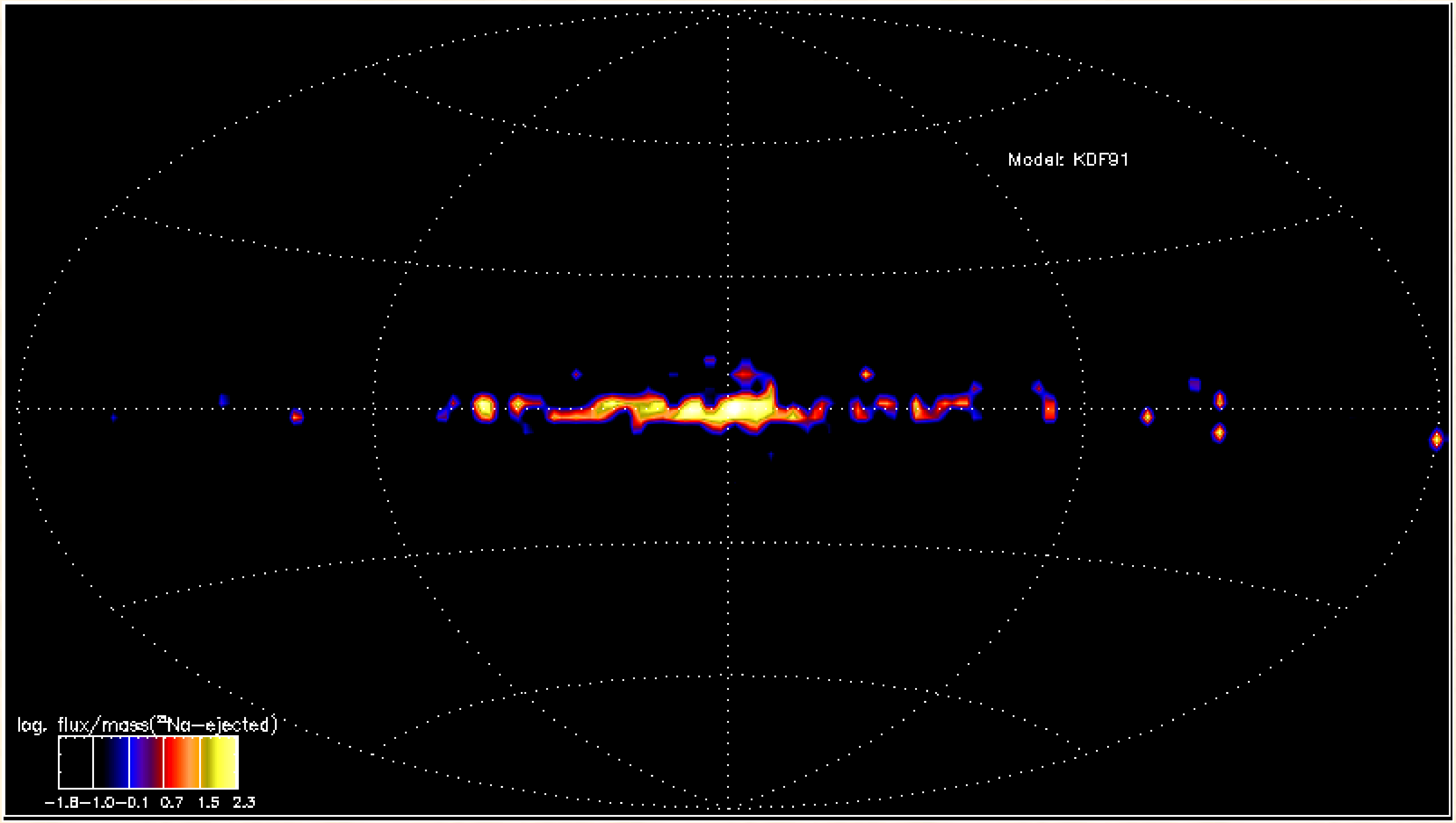

Theoretical predictions:Jean, Hernanz, Gómez-Gomar, José, 2000, MNRAS

Observations (upper limits): Leising et al. 1988, Harris et al 1991, 1996

^{26}Al ejected masses by ONe novae
Nuclear uncertainties

WD mass	Minimum	Best	Maximum	Max/Min
1.15	$8.6 \cdot 10^{-9}$	$2.1 \cdot 10^{-8}$	$3.1 \cdot 10^{-8}$	3.6
1.25	$3.6 \cdot 10^{-9}$	$1.2 \cdot 10^{-8}$	$1.6 \cdot 10^{-8}$	4.4
1.35	$6.6 \cdot 10^{-10}$	$3.2 \cdot 10^{-9}$	$4.8 \cdot 10^{-9}$	7.3

(all in $M_\odot$)

José, Coc and Hernanz 1999, ApJ

Contribution of novae to Galactic ^{26}Al:

$M(^{26}Al) \approx 2.0\ M_\odot * M_{ej}(^{26}Al)/(10^{-7}\ M_\odot) * R_N/(35\ yr^{-1}) * f_{ONe}/0.5 \sim 0.4\ M_\odot$

$< M(^{26}Al)$ from CGRO/COMPTEL 1809 keV map

Need of more sensitive intruments

Future missions

- MAX (γ-ray lens),
- ACT (Advanced Compton Telescope)

Why focusing γ-rays?

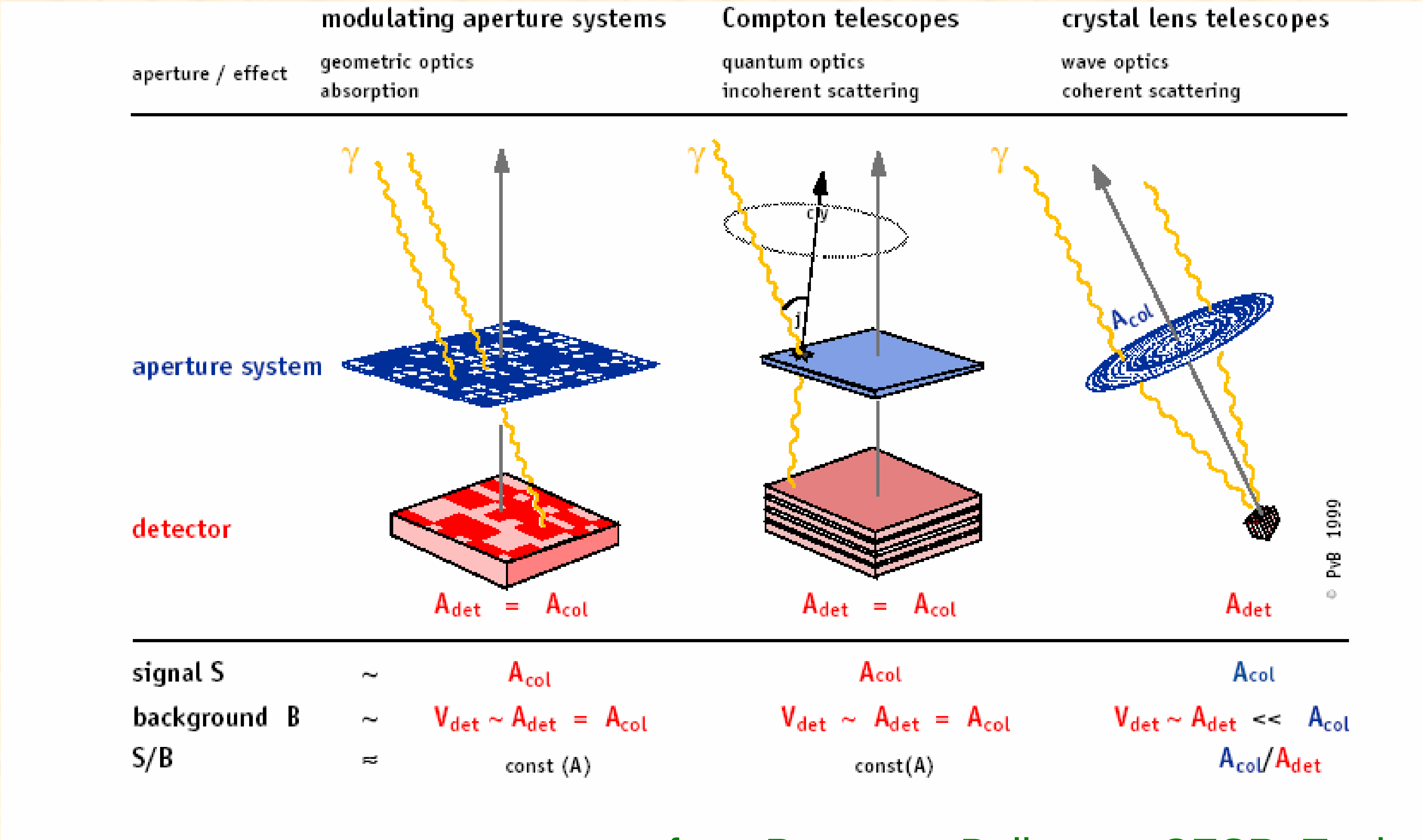

from Peter von Ballmoos, CESR, Toulouse

How to focus γ-rays?

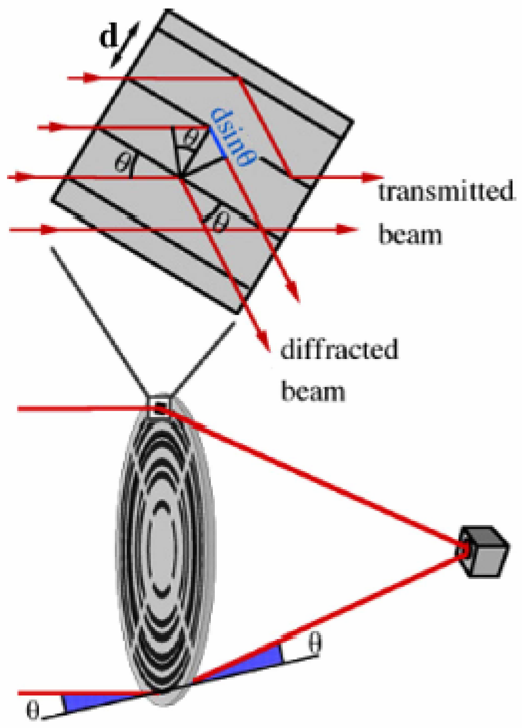

λ(511 keV)	=	$2.42632 \cdot 10^{-2}$ Å

Bragg condition

$2d\sin\theta$	=	$n\lambda$

d[220]	=	2.0004Å
arcsin(λ/2d)	=	0.347°

Laue-type Gamma-ray lens

2θ	=	0.695°
ex. radius [220]	=	10.1 cm
=> focal lenght	=	8.2 m

http://www.cesr.fr/~pvb/Claire/index.html

A gamma-ray lens for nuclear astrophysics

http://www.cesr.fr/~pvb/Claire/index.html

Is the lens performing as expected for sources at infinity?

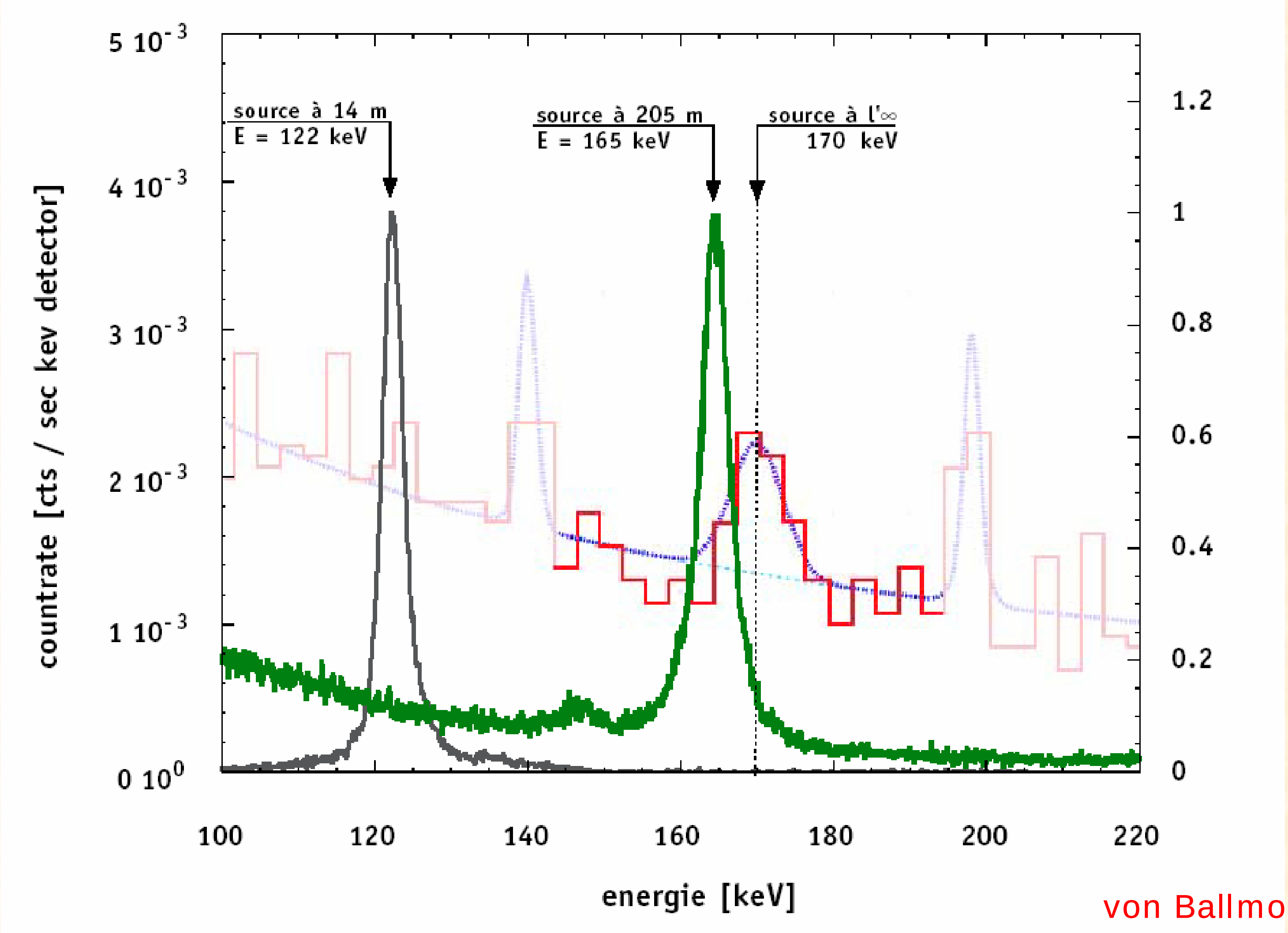

von Ballmoos et al. 2004.

From CLAIRE to MAX (space mission)

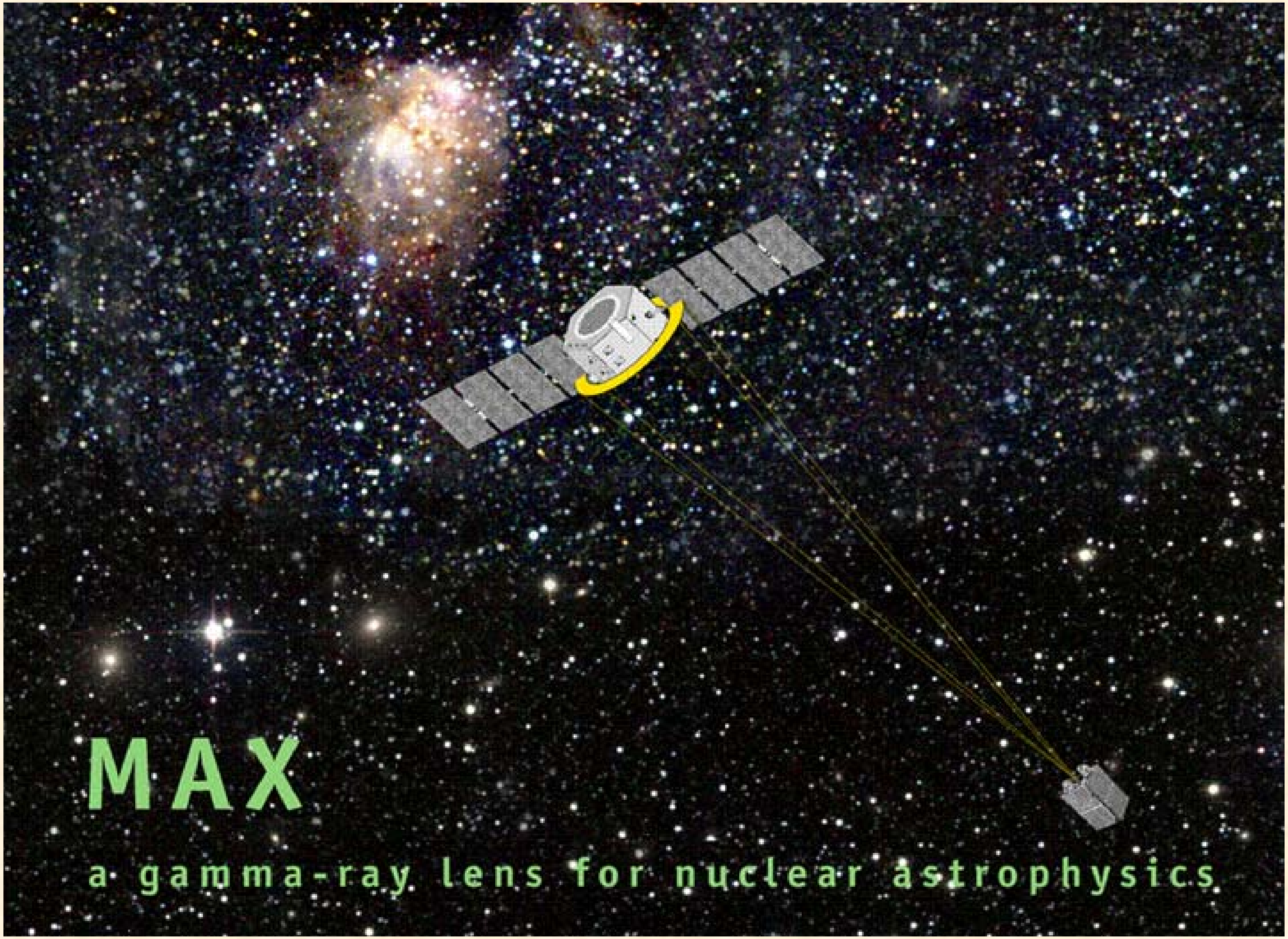

www.cesr.fr/~pvb/MAX/

two 100 keV broad energy bands diffracting simultaneously

MAX

inner radius	86 cm
outer radius	111 cm
focal length	133 m

MAX XL

inner radius	193 cm
outer radius	250 cm
focal length	300 m

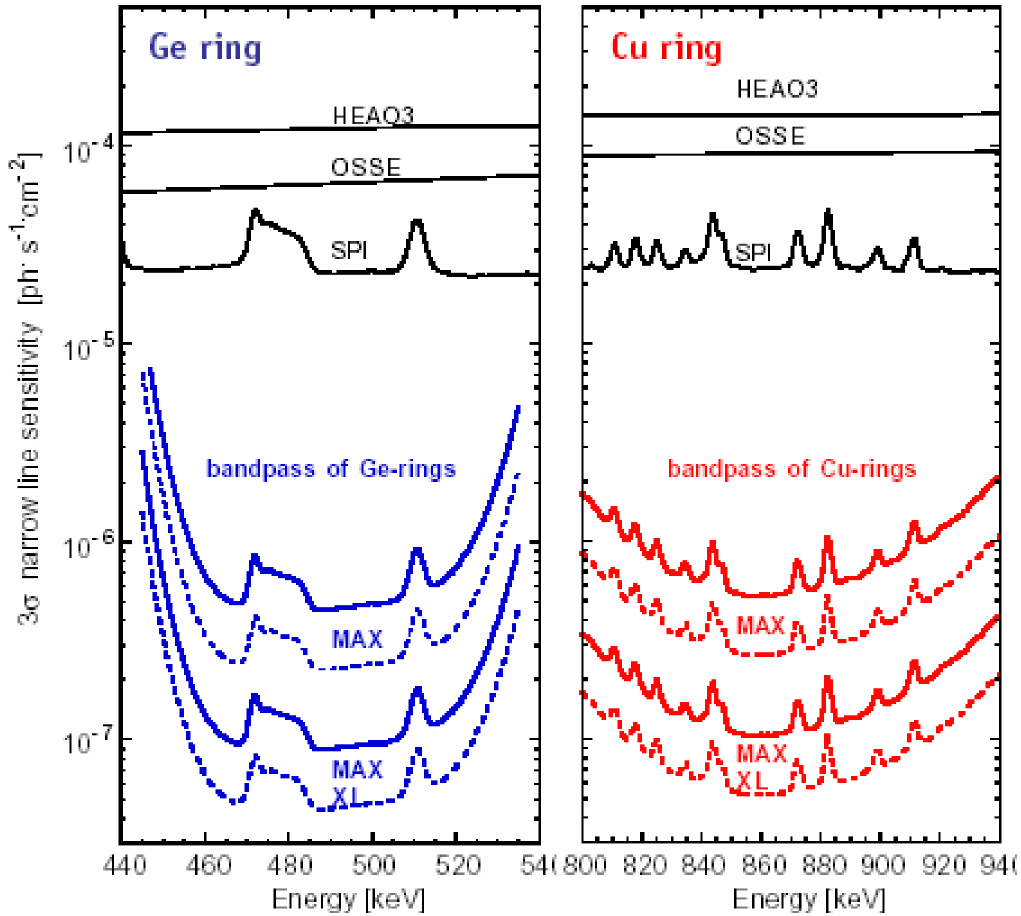

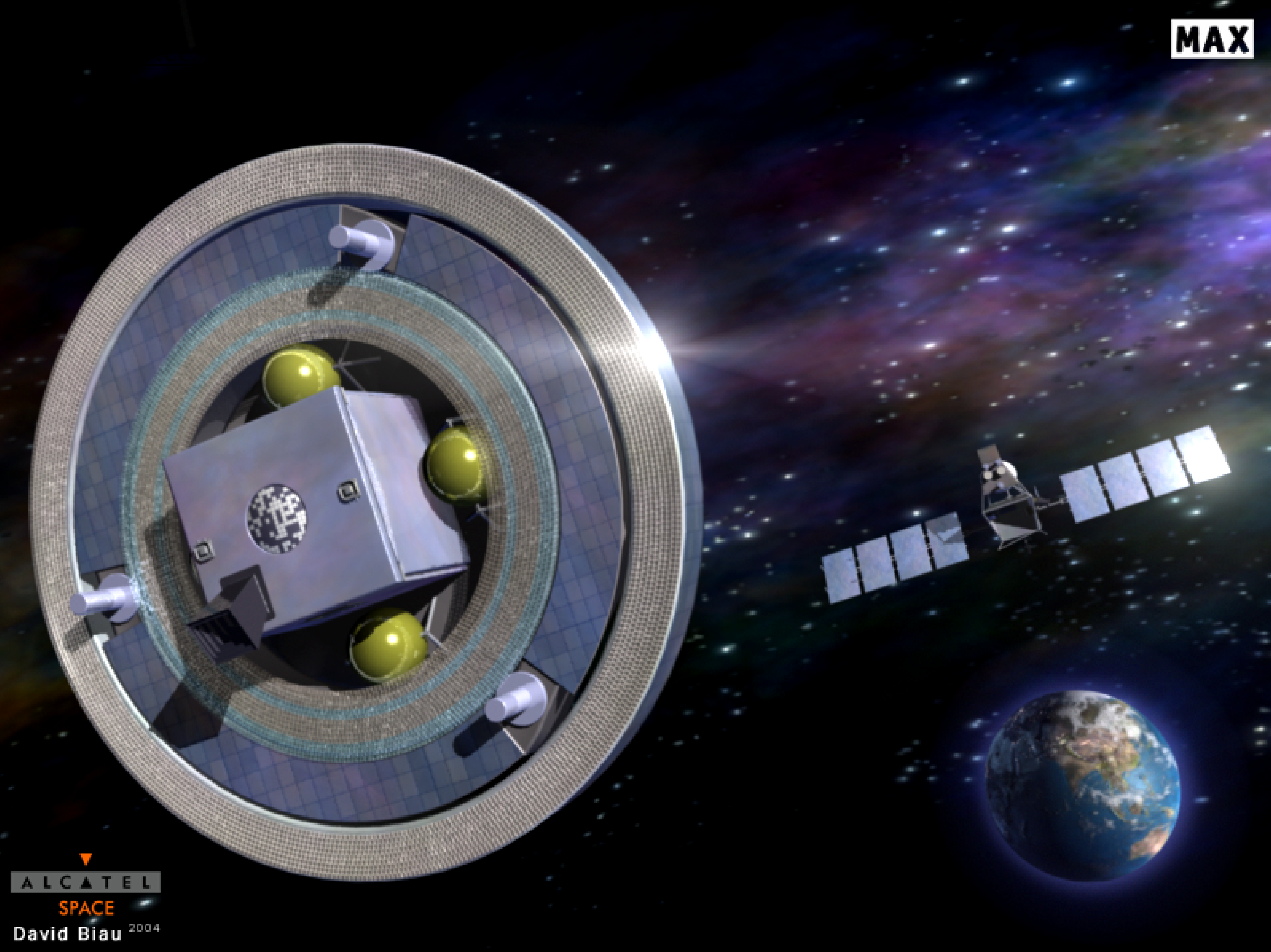
MAX
ALCATEL
SPACE
David Biau 2004

Summary

- White dwarf mass and chemical composition are not independent variables: CO (M<8-10 $M_\odot$) and ONe ((8-10) $M_\odot$ <M< 12 $M_\odot$).
- Need of core-envelope mixing to explain both the explosion itself and the observed ejecta abundances. Not self-consistent mechanism found to date.
- Observational diagnostics of nova nucleosynthesis: particular novae, isotopic abundances in meteorites, chemical evolution of the Galaxy, gamma-ray emission. Gamma-rays could provide infomation about the distribution of novae in the Galaxy, avoiding the problem of interstellar extinction.